



1 **Methanogenesis by CO₂ reduction dominates lake sediments** 2 **with different organic matter compositions**

3
4 Guangyi Su^{1*}, Julie Tolu², Clemens Glombitza³, Jakob Zopfi⁴, Moritz F. Lehmann⁴,
5 Mark A. Lever³, Carsten J. Schubert^{1, 3}

6
7 ¹ Swiss Federal Institute of Aquatic Science and Technology (EAWAG), Department of Surface
8 Waters – Research and Management, 6047 Kastanienbaum, Switzerland

9 ² Swiss Federal Institute of Aquatic Science and Technology (EAWAG), Department of Water
10 resources and Drinking water, 8600 Duebendorf, Switzerland

11 ³ Institute of Biogeochemistry and Pollutant Dynamics, ETH Zurich, 8092 Zurich, Switzerland

12 ⁴ Department of Environmental Sciences, University of Basel, 4056 Basel, Switzerland

13
14 *corresponding author: Guangyi Su, guangyi.su@unibas.ch

15 16 17 **Abstract**

18 Microbial methane production is a respiration reaction involved in the terminal
19 step of anaerobic degradation of organic matter. Due to the dependency of
20 methanogenic substrate production on fermentation reactions that produce different end
21 productions, different sources and compositions of organic carbon (OC) may impact
22 the methanogenic potential in lake sediments. Here, we investigate the sources and
23 compositions of OC in sediments of Lake Geneva and how both are potentially linked
24 to methane production. Differences in dominant long-chain fatty acid abundances and
25 carbon isotopic compositions suggest the predominance of diagenetically altered
26 phytoplankton-derived OC at a profundal site and temporally highly variable sources
27 of both aquatic and terrestrial OC in a deltaic location. Despite these differences,
28 radiotracer-based methanogenesis rate measurements and stable isotopic signatures of
29 methane indicate significant methane production that is dominated by CO₂ reduction
30 (>95% of total methanogenesis) in both locations. Matching this interpretation,
31 members of well-known CO₂-reducing *Methanoregula* sp. dominate both sites. No
32 clear effect of OC source on methane production rates was evident. Our data
33 demonstrate that OC of diverse sources and diagenetic states support microbial methane
34 production, but do not indicate a clear impact of the OC source on the dominant
35 methanogenic pathway or the community structure of methanogenic microorganisms
36 in lacustrine sediments.



37

38 Keywords: Methane production rate; Methanogenesis pathway; Sediment organic
39 carbon; Lipid biomarkers; Methanogen community

40

41 1. Introduction

42 Lakes represent an important source of methane (CH_4) to the atmosphere
43 (Bastviken et al., 2011), which is a potent greenhouse gas with a global warming
44 potential more than 27 times that of carbon dioxide on a 100-year basis (GWP-100)
45 (Masson-Delmotte et al., 2021). A large fraction of CH_4 produced in lakes is produced
46 during the anaerobic decomposition of organic carbon (OC) in sediments, from where
47 it escapes by ebullition or diffusion into the bottom waters. Methane formation is the
48 final step in the degradation of organic matter, and is catalyzed by anaerobic
49 methanogenic archaea, capable of using several substrates including H_2/CO_2 , acetate,
50 and methylated compounds (Lyu et al., 2018). It is still poorly understood how methane
51 production in lake sediments is regulated, and to what extent the methanogenic
52 potential is related to OC quality. In this regard, microbial organic matter degradation
53 reactions (e.g., hydrolysis, fermentation, and anaerobic oxidation) play a critical role
54 by sequentially breaking down organic macromolecules, such as proteins,
55 carbohydrates, and lipids, to acetate and H_2/CO_2 , which are then used as substrates by
56 methanogenic archaea (Demirel and Scherer, 2008).

57 Freshwater lakes cover only a small portion of the Earth's surface ($< 3\%$)
58 (Downing et al., 2006), compared to oceans (71%), yet, the annually accumulated OC
59 in lakes represents nearly half of what is stored in the oceans (Mendonça et al., 2017).
60 In many lakes, most of organic matter in sediments is derived from autochthonous
61 aquatic organisms like phytoplankton and aquatic macrophytes (Dean and Gorham,
62 1998). On the other hand, allochthonous organic carbon such as detritus of terrestrial
63 vegetation can account for a significant fraction of the lacustrine sedimentary organic
64 matter (Larsen et al., 2011), for example within river deltas (Randlett et al., 2015). In
65 small or oligotrophic lakes and/or high-latitude/altitude lakes, OC sedimentation may
66 in fact be dominated by land-derived organic matter, and it has previously been
67 observed that high carbon burial efficiency in sediments is linked to a high proportion
68 of allochthonous OC (Sobek et al., 2009). In general, OC from aquatic biomass such as
69 phytoplankton mainly comprises relatively labile compounds (Parsons et al., 1961). In



70 contrast, allochthonous OC (e.g., terrestrial plants) contains more complex structural
 71 and biochemically recalcitrant compounds, such as cellulose and lignin (Opsahl and
 72 Benner, 1995), which are more effectively preserved over time (Han et al., 2020, 2022).
 73 The different biochemical compositions and characteristics of OC in lake sediments,
 74 and the associated differential susceptibility to hydrolytic attack and microbial
 75 breakdown into smaller carbon compounds (Lehmann et al., 2002a, 2020), might
 76 substantially affect CH₄ production and emission, as has been suggested in previous
 77 studies (Grasset et al., 2018; West et al., 2012). However, laboratory experiments
 78 performed at short-time scales (i.e., within weeks or months), involving the spiking of
 79 sediments with fresh algal and/or plant organic materials, do not accurately reflect
 80 effects of enhanced OC contribution to natural sediments on CH₄ production because
 81 the compositions and lability of original organic materials may vary greatly after
 82 sedimentation due to oxidative destruction and microbial alteration during sinking in
 83 the water column (Kawamura et al., 1987). Moreover, allochthonous OC found in lake
 84 sediments is often the less-reactive (i.e. less bio-degradable) remnant of land-derived
 85 debris, where the more reactive fractions have already been removed on land or during
 86 fluvial transport (Raymond and Bauer, 2001). Lastly, while it is known that organic
 87 matter bioavailability decreases over time, as labile components are selectively
 88 remineralized (Grasset et al., 2018), the effects of organic matter quality and OC
 89 degradation state, and their interactions, on CH₄ production remain uncertain.

90 Lipid biomarkers and their stable carbon isotopic composition can be used to infer
 91 sources and diagenetic state of lacustrine organic matter (Dai et al., 2005; Meyers and
 92 Ishiwatari, 1993). Different chain lengths of fatty acids and n-alkanes can be used for
 93 the distinction between aquatic phytoplankton and terrestrial plants (Cranwell, 1976;
 94 Eglinton and Hamilton, 1967). In addition, primary producers growing in different
 95 habitats (e.g., terrestrial plants and freshwater phytoplankton) have distinct isotopic
 96 compositions, due to the differences in C sources and biochemical pathways, through
 97 which inorganic carbon is assimilated and incorporated into biomass (Cloern et al.,
 98 2002). For example, terrestrial plants incorporate carbon dioxide from the atmosphere
 99 using the C₃ Calvin-Benson pathway and consequently have an average bulk isotopic
 100 value of ca -28‰, while isotopic values of various aquatic plants are often significantly
 101 less negative (e.g., an average of -20‰ for benthic diatoms) (Cloern et al., 2002;
 102 O’Leary, 1981). Moreover, stable carbon isotope measurements can be used to trace
 103 the carbon flow from organic matter degradation to CH₄ in lake sediments. The isotopic



signatures of methane and methane precursors (e.g., dissolved inorganic carbon, bulk organic carbon) can be used to assess the relative contribution of the major pathways (i.e., hydrogenotrophic and acetoclastic methanogenesis) to total CH₄ production (Conrad, 2005; Whiticar, 1999). To date it remains unclear, which organic compounds represent the main precursors of molecules that are ultimately converted to methane in older sediments, in which more labile OC fractions, such as OC from microalgal cells, have largely been remineralized already. Previous research in Lake Geneva revealed higher benthic CH₄ fluxes, but lower total mineralization rates of organic matter in deltaic sediments, compared to profundal sites with reduced riverine impact (Randlett et al., 2015). The observed differences imply that despite less efficient total remineralization that leads to elevated OC burial rates in deltaic sediments, high CH₄ production is sustained due to the high input of allochthonous OC (Sollberger et al., 2014).

Here we investigated relationships between methanogenesis rates and pathways, and the sources and degradation state of sedimentary organic matter in profundal and deltaic sediments of Lake Geneva. We combined methanogenic rate measurements by radiotracer incubations with ¹⁴C-labeled bicarbonate and acetate with compositional (lipids, pyrolysis-GC/MS) and stable carbon isotopic analyses of organic carbon and CH₄, and sedimentation rate measurements (based on Pb-210, Cs-137). Additional quantitative analyses of a methanogenic marker gene (*mcrA*) and analyses of methanogenic community structure (16S rRNA gene sequences) provided insights into the abundances and identities of in situ methanogenic populations. Based on this multi-disciplinary data set, we identified potential relationships between sediment OC sources and degradation status, rates, pathways, and the organisms involved in the microbial production of methane.

2. Material and methods

2.1. Study sites

Lake Geneva is the largest western European lake. The Rhone River, the main tributary to the lake in the northeastern part, has a catchment area of 5220 km² and accounts for about 68% of the total water discharge and large amounts of suspended sediment and fine-particle loading to the lake (Burrus et al., 1989). The Rhone River inflow brings in large amounts of terrestrial OC, which is mostly deposited near the



137 river mouth as an important contribution to deltaic sediments. On the other hand,
 138 sedimentation in the deeper part of the lake is usually dominated by phytoplankton-
 139 derived OC (Gallina et al., 2017).

140

141 **2.2. Sample collection and processing**

142 Sediment cores were collected using a larger gravity corer (14 cm inner diameter)
 143 at a profundal site (46°25'54"N, 6°47'33"E, water depth: 240 m) and a smaller gravity
 144 corer (6.5 cm inner diameter) at a deltaic site (46°24'58"N, 6°51'34"E, water depth: 128
 145 m) in August and December 2019, respectively. Profundal samples for different
 146 analyses were obtained from a single sediment core at 2-cm vertical resolution. Samples
 147 for the analysis of dissolved methane concentrations were collected on site with cut-off
 148 syringes through pre-drilled holes in the core liner covered with adhesive tape.
 149 Sediment samples of 2 cm³ were fixed with 5 mL 10% NaOH in 120 mL serum bottles,
 150 which were capped immediately with thick butyl rubber stoppers and an aluminum
 151 crimp cap. Additionally, two replicate samples were taken from the same depth for
 152 methanogenesis rate measurements (described below). Sediment porewater was
 153 extracted with Rhizon samplers (Rhizosphere Research Products, Wageningen,
 154 Netherlands) connected to 20-mL syringes through predrilled small holes, with 2 cm
 155 distance between them. Porewater samples for DIC concentration measurements and
 156 stable carbon isotope analyses were stored in 4-mL glass vials without headspace at 4
 157 °C. Separate porewater sample aliquots for the quantification of acetate and other
 158 volatile fatty acids were stored in combusted (450 °C for 5 h) glass vials at -20 °C until
 159 further analysis. The sediment core was then extruded in the lab and sectioned into 2
 160 cm segments. Samples were taken from each segment and stored frozen (-20 °C) until
 161 further analysis for bulk parameters and lipid biomarkers. Using the gravity corer
 162 equipped with the smaller core liner, four sediment cores were obtained from the deltaic
 163 site. One core was used for methane concentration measurements, a second one for rate
 164 measurements (both at 2-cm resolution, sample collection as described above). The
 165 third core was used for porewater extraction in the lab using Rhizon samplers, and the
 166 last one was split open for the determination of porosity, analysis of bulk parameters
 167 and lipid biomarkers. An additional small-diameter sediment core was taken at the
 168 profundal site during the second sampling campaign for porosity analysis.

169

170 **2.3. Rate measurements of methanogenesis using radiolabeled substrates**



171 Methanogenesis rates (MGR) were determined using a radioisotope-based
 172 approach. We determined the modes of methane production and activity rates in
 173 incubation experiments with radio-labeled acetate and bicarbonate. At each depth,
 174 samples (2.5 cm³) were collected through pre-drilled holes using 3 mL cut-off plastic
 175 syringes, which were closed with rubber stoppers and stored at 4 °C. Upon arrival of
 176 the samples in the laboratory, ten microliters of anoxic ¹⁴C-labeled bicarbonate (~16
 177 kBq, Perkin-Elmer) or 2-¹⁴C-labeled (i.e., ¹⁴C label in the carboxyl group) acetate
 178 solution (~18 kBq, Perkin-Elmer) were injected for the MGR measurements to
 179 determine hydrogenotrophic (MGR_{DIC}) and acetoclastic (MGR_{Ac}) methanogenesis
 180 rates, respectively. Immediately after the tracer injection through the stoppers, all
 181 samples including killed controls (i.e., samples that were transferred to 10 mL 5%
 182 NaOH solution immediately after tracer injection) were incubated under an N₂
 183 atmosphere at in situ temperature (4 °C) in the dark for 48 h.

184 To stop microbial activity in the incubations with ¹⁴C-labeled substrates, samples
 185 were transferred into 120-mL serum bottles containing 10 mL aqueous NaOH (5%
 186 wt:wt), immediately crimp-sealed with butyl rubber stoppers and vigorously shaken.
 187 The ¹⁴C activity in the different carbon pools was determined as previously described
 188 (Su et al., 2019). In brief, the headspace of a fixed sample is purged with air (30 mL
 189 min⁻¹ for 30 min) through a heated (850 °C) quartz tube filled with copper oxide, where
 190 the ¹⁴CH₄ (product of methanogenesis during incubation) is combusted to ¹⁴CO₂. The
 191 ¹⁴CO₂ is then captured in two sequential traps of scintillation vials (20 mL) containing
 192 8 mL of 1:7 phenylethylamine and methoxyethanol. The cumulative radioactivity of
 193 both traps is then determined by liquid scintillation counting (2200CA Tri-Carb Liquid
 194 Scintillation Analyzer) after adding 8 mL of a scintillation cocktail (Ultima Gold,
 195 PerkinElmer) to each vial, and thorough mixing using a vortex-mixer. For incubations
 196 with bicarbonate, the residual ¹⁴C-bicarbonate was measured as ¹⁴CO₂, released from
 197 the alkaline liquid phase after adding 2.5 mL of 32% HCl. The remaining radioactivity
 198 (possibly explained by inorganic carbon assimilation into biomass) was determined in
 199 a 1-mL aliquot of the acidified mixture (amended with 4 mL Ultima Gold) by liquid
 200 scintillation counting. Incubation bottles with ¹⁴C-acetate were also acidified with 2.5
 201 mL of 32% HCl after extraction of ¹⁴CH₄, and ¹⁴CO₂ from microbial acetate oxidation
 202 was subsequently purged and trapped as described above. To determine the residual
 203 ¹⁴C-acetate in the incubation vial, 1 mL of the acidified mixture was mixed with 4 mL
 204 Ultima Gold for scintillation counting (Beulig et al., 2018). The control samples were



processed in the same way as the incubated samples after the termination of incubation. The methanogenesis rates with DIC ($\text{nmol cm}^{-3} \text{ d}^{-1}$) and acetate ($\text{nmol cm}^{-3} \text{ d}^{-1}$) as substrates were calculated using Eq. 1 and Eq. 2, respectively, modified from a previous study (Beulig et al., 2018).

$$MGR_{DIC} = 1.08 \times \varphi \times [DIC] \times \frac{A_{CH_4}}{A_{CH_4} + A_{DIC} + A_R} \times t^{-1} \quad (1)$$

$$MGR_{Ac} = 1.08 \times \varphi \times [Ac] \times \frac{A_{CH_4}}{A_{CH_4} + A_{DIC} + A_{Ac}} \times t^{-1} \quad (2)$$

$[DIC]$ and $[Ac]$ are concentrations of DIC and acetate in the sediment porewater, respectively. A_{CH_4} and A_{DIC} represent the activities of produced CH_4 and DIC (i.e., residual DIC in bicarbonate-amended incubations, product DIC in acetate-amended incubations) at the end of the incubation (in CPM). A_R and A_{Ac} represent the remaining radioactivity of DIC-incubated samples (i.e., biomass and metabolic intermediates) and the residual ^{14}C -acetate radioactivity (possibly also including a small fraction of ^{14}C in metabolic intermediates and incorporated into biomass), respectively. φ is the porosity of the sediment samples. The factor 1.08 accounts for the isotopic fractionation of ^{14}C (Hansen et al., 2001). t represents the incubation time in days. Measured $^{14}\text{CH}_4$ activities in all incubation samples were blank-corrected by subtracting the $^{14}\text{CH}_4$ activity measured in the killed control (typically close to background radioactivity) incubated with the same amounts of ^{14}C -labeled substrates. The activities in the $^{14}\text{CH}_4$ pool were considered zero if the blank-corrected value was negative.

2.4. Pore water methane and nutrient analyses

Methane concentrations were measured in the headspace of NaOH-preserved samples using a gas chromatograph (GC, Agilent 6890N) with a flame ionization detector, and helium as a carrier gas. CH_4 concentrations in the wet sediments were then calculated based on the headspace-to-sample volume ratio. The C isotopic composition ($^{13}\text{C}/^{12}\text{C}$) of methane was determined in the same samples using a pre-concentration unit (TraceGas, Micromass, UK) connected to an isotope ratio mass spectrometer (IRMS; GV Instruments, Isoprime). Stable C-isotope values are reported in the conventional δ notation (in ‰) relative to the Vienna Pee Dee Belemnite standard (V-PDB), with a reproducibility of 0.5‰ based on replicate measurements of methane standards. A carbon analyzer (TOC-L, Shimadzu, Kyoto, Japan) was used to quantify dissolved inorganic carbon (DIC) concentrations in sediment porewaters. Samples were



manually injected into the DIC reaction vessel and measured with a non-dispersive infrared detector (NDIR) after acidification and volatilization to CO₂. To determine the carbon isotopic composition of DIC, a porewater aliquot of 1-2 mL was introduced into a He-purged exetainer (Labco Ltd) and acidified with ~200 µL 85% H₃PO₄. After 2 h equilibration at 37 °C, the CO₂ released from the aqueous phase was subsequently analyzed using a preparation system (MultiFlow, Isoprime) coupled to an IRMS (Micromass, Isoprime). The standard deviation for replicate measurements of samples and standards was < 0.2‰. Porewater samples for acetate and other volatile fatty acids were analyzed with a two-dimensional ion chromatography (2D IC), as described previously (Glombitza et al., 2014), with modifications reported in (Schaedler et al., 2018). Samples were filtered through pre-washed (10 mL Ultrapure Type I water) disposable syringe filters (Acrodisc® IC grade, 0.2 µm pore size, 13 mm diameter). The first 0.5 mL sample after filtration was discarded before collecting the samples for 2D IC analysis. We used a dual Dionex ICS6000 instrument (Thermo Scientific) equipped with a Dionex AS24 column (2 mm diameter) for the first dimension, and a Dionex AS11HC column (2 mm diameter) for the second dimension. Quantification was done from the conductivity detector signal with a series of 5 external standards between 0.5 and 100 µM.

2.5. Bulk sediment analyses

The total organic carbon (TOC) contents of sediment samples were determined by the difference between total carbon and total inorganic carbon. Samples for total carbon were measured with an Elementar Vario Pyro Cube CN elemental analyser (Elementar, Germany), and samples for total inorganic carbon were analysed by coulometry using a UIC CM5015 coulometer (Joliet, IL, USA). Sediment cores were dated by gamma spectrometry using ¹³⁷Cs on freeze-dried and ground sediment for the determination of sedimentation rates, as described previously (Randlett et al., 2015). The δ¹³C-TOC was determined on decalcified samples (Schubert and Nielsen, 2000). Briefly, freeze-dried and homogenized samples were treated with 5 mL 10% HCl in 15 mL Falcon tubes overnight. After centrifugation, the supernatant was discarded, and the solid phase was washed/centrifuged three times with 5 mL MilliQ water. Samples were dried at 50 °C for 48 h prior to analysis. The δ¹³C-TOC was then assessed by elemental analysis-isotope ratio mass spectrometry (EA, Pyro Cube, Elementar and IRMS, Isoprime, UK).



270 The reproducibility based on replicate measurements of standards and samples was
271 better than 0.2%.

272

273 **2.6. Pyrolysis gas chromatography-mass spectrometry**

274 The sedimentary organic matter composition was characterized at the molecular
275 level using a pyrolyzer equipped with an autosampler (EGA/PY-3030D and AS-1020E,
276 FrontierLabs, Japan) connected to a gas chromatograph (Trace 1310, Thermo
277 Scientific) and a mass spectrometer (ISQ 7000, Thermo Scientific), following the
278 optimized method (Tolu et al., 2015). Depending on the sample, an aliquot of 2-3 mg
279 of dry sediment was pyrolyzed at 450°C. A data-processing pipeline, including
280 chromatogram smoothing, alignment background correction and multivariate curve
281 resolution by alternate regression was used to automatically detect and integrate the
282 peaks and extract their mass spectra under “R” computational environment (R Core
283 Team 2014). To optimize the number of detected peaks, data processing was performed
284 independently for the sediments from the deltaic site (DS) and the profundal site (PS).
285 Individual peaks were identified using “NIST MS Search 2” software which includes
286 the library “NIST/EPA/NIH 2011”, complemented by spectra from published studies.
287 The relative abundances of these identified pyrolytic organic compounds were
288 calculated for each sample by normalization to the sum of their peak areas set at 100%.

289

290 **2.7. Lipid extraction, separation, and quantification**

291 Based on methanogenesis rate and geochemical profiles, sediment samples from
292 five selected depths of both locations were lyophilized and homogenized for subsequent
293 lipid extraction. Prior to extraction, an internal standard mix (5 α -androsterane, 3-
294 eicosanone, n-C19:0 fatty acid and n-C19 alkanol) was added to each sample for the
295 quantification of single biomarkers. Lipids were extracted in 20 mL of 7:3
296 Dichloromethane/Methanol (DCM/MeOH) in a Microwave Reaction System (SolvPro,
297 Anton Paar, Graz, Austria), as described previously (Ladd et al., 2018). Total lipid
298 extracts (TLEs) were obtained by successively rinsing the samples with DCM after
299 centrifugation, and then concentrated using a Multivapor P-6 (Büchi Labortechnik AG,
300 Switzerland). TLEs were further evaporated to dryness, and saponified in 3 mL
301 methanolic KOH-solution (~1 N) at 80 °C for 3 h. Neutral compounds were extracted
302 by liquid-liquid extraction using hexane, fatty acids (FAs) were then extracted from the
303 remaining aqueous phase with hexane after acidification (pH < 2). The fatty acid



fraction was treated using 1 mL of BF_3 in methanol (14% v/v, Sigma Aldrich) at 80 °C for 2 h, and converted to fatty acid methyl esters (FAMES). Neutral compounds were further separated into four different fractions using 500 mg/6mL pre-packed Si gel columns (filling quantity/volume, Biotage, Uppsala, Sweden). Briefly, the neutral fraction was dissolved in 4 mL hexane and transferred onto the column, followed by 4 mL hexane/DCM (2:1 v/v), then 4 mL DCM/MeOH (19:1 v/v) and finally 4 mL MeOH, with the elution of hydrocarbon, ketone, alcohol and remaining polar compounds, respectively. The alcohol fraction was acetylated in 25 μL acetic anhydride and 200 μL pyridine at 70 °C for 30 min.

All fractions were quantified using a gas chromatograph equipped with a flame ionization detector (GC-FID) (GC-2010 Plus, Shimadzu, Japan). Samples were injected onto an InertCap 5MS/NP column (0.25 mm \times 30 m \times 0.25 μm , GL Sciences, Japan) using an AOC-20i autosampler (Shimadzu) through a split/splitless injector operated in splitless mode at 280 °C. The column was heated from 70 °C to 130 °C at 20 °C min^{-1} , then to 320 °C at 4 °C min^{-1} , and held at 320 °C for 20 min. FAMES were identified by comparing their retention times to those of laboratory standards (i.e., a fatty acid methyl ester mix and bacterial acid methyl ester from Supelco, reference no. 47885-U and 47080-U, respectively), and were quantified by normalization to the internal n-C19:0 fatty acid standard. Identification of hydrocarbons was performed by comparing their retention times to those of an external standard containing C14 to C40 n-alkanes (Sigma-Aldrich). The alcohols were characterized using a gas chromatography-mass spectrometer (GC-MS, QP2020, Shimadzu, Japan) under identical chromatographic conditions. Acquired mass spectra were identified through comparison with published data.

2.8. Compound-specific stable carbon isotope analysis

The stable carbon isotope composition of FAMES, n-alkanes and alcohols was determined by gas chromatography-isotope ratio mass spectrometry (GC-IRMS), using a Delta V Advantage IRMS (Thermo Scientific) with a ConFlow IV (Thermo Scientific). Samples were injected with a TriPlus RSH autosampler to a PTV inlet operated in splitless mode at 280 °C on a GC-1310 gas chromatograph (Thermo Scientific, Bremen, Germany). The GC was equipped with a 30 m DB-5MS fused silica capillary column (0.25 mm i.d., 0.25 μm film thickness). The GC oven was heated from 80 °C to 215 °C at 15 °C min^{-1} , then to 320 °C at 5 °C min^{-1} , and held at 320 °C for 10



min. Column effluent was combusted at 1020 °C. Compound-specific $\delta^{13}\text{C}$ values were reported relative to the V-PDB scale, and calibrated externally using known $\delta^{13}\text{C}$ values of an alkane mixture (n-C₁₇, 19, 21, 23, 25, 28 and 34, Arndt Schimmelmann, Indiana University, USA), which were run at the beginning and the end of each sequence, as well as after every 6th sample injection. The standard deviation for replicate measurements for these standards averaged 0.4‰, with the average offset from their known values of less than 0.5‰. The isotopic values of FAMES and acetylated alcohols were additionally corrected for the introduction of carbon atoms during the derivatization step.

2.9. DNA extraction, PCR amplification, Illumina sequencing and data analysis

DNA was extracted from selected sediment samples of Lake Geneva, where high methanogenic rates were detected (see below), using FastDNA SPIN Kit for Soils (MP Biomedicals) following the manufacturer's instructions. A two-step PCR approach was applied to prepare the library for Illumina sequencing at the Genomics Facility Basel, as described in detail previously (Su et al., 2020, 2023). PCR was performed using universal primers 515F-Y and 926R targeting the V4 and V5 regions of the 16S rRNA gene. These primers cover the majority (~84.7%) of the 16S rRNA gene sequences of methanogenic archaea and are well-suited for assessing community structures of methanogens in environmental samples (Table S4). Data were then analyzed with Phyloseq (McMurdie and Holmes, 2013) in the R environment (R Core Team 2014). Raw sequence data were deposited at NCBI Short Read Archive under the Bioproject ID PRJNA736863 with accession numbers from SAMN19667760 to SAMN19667767.

2.10. Quantitative PCR (qPCR)

The abundance of methanogens in Geneva sediments was determined by qPCR with the primer set mcrIRD and 2 µL DNA as template (Lever and Teske, 2015). qPCR reactions of all DNA samples were performed using the SensiFAST SYBR No-ROX Kit (Bioline) on a Mic (Magnetic Induction Cycler) real time PCR machine (Bio Molecular Systems, Inc). An initial denaturing step of 95 °C for 3 min was followed by 40 cycles of 5 s at 95 °C, 10 s at 56 °C, and 22 s at 72 °C. The specificity of the amplification was assessed by examining the melting curves from 72 °C to 95 °C. The calibration curve was generated using a serial of 10-fold dilutions of pGEM-T Easy plasmid DNA (Promega, USA) carrying a single copy of the target gene (mcrIRD-



F/mcrIRD-R). The number of gene copies in plasmid DNA was calculated using the equation reported previously (Ritalahti et al., 2006).

3. Results

3.1. Sediment geochemistry at the two study sites

The two sites displayed different hydro- and geochemical characteristics (Fig. 1 and Table S1 and Fig. S1). Dating of the sediments revealed that the deltaic site had a slightly higher sedimentation rate (0.58 cm yr^{-1}) than the profundal site (0.43 cm yr^{-1}). At the deltaic site (DS), two distinct peaks in methane concentration ($\sim 7 \text{ mM}$) were observed at 9 and 23 cm, respectively (Fig. 1A). At the profundal site (PS), concentrations of CH_4 increased with depth and remained relatively constant at $\sim 4 \text{ mM}$ below 15 cm (Fig. 1E). At both sites, the pore water concentrations of dissolved inorganic carbon (DIC) increased with depth, and considerable amounts accumulated in the sediment pore water. The depth-integrated DIC concentrations in the top 30 cm were 1964 mmol m^{-2} at PS and 3490 mmol m^{-2} at DS, however, based on the sedimentation over the past 50 years, the depth-integrated DIC concentrations were 1302 mmol m^{-2} at PS (21 cm) and 3490 mmol m^{-2} at DS (29 cm). Acetate, as a potential methanogenic substrate, showed concentration maxima of $25.9 \text{ }\mu\text{M}$ (DS) and $3.8 \text{ }\mu\text{M}$ (PS) close to the sediment surface. The methane $\delta^{13}\text{C}$ values decreased with depth in both deltaic sediments (from -64.9‰ to -72.2‰ , Fig. 1B) and profundal sediments (from -72.7‰ to -74.6‰ , Fig. 1F). Overall, the observed methane carbon isotope values at both sites fall within a range that is typical for biogenic production (Whiticar, 1999). Vertical profiles of $\delta^{13}\text{C}$ -DIC show similar pattern at the two sites, with the lowest values of -5.5‰ at 5 cm at DS (Fig. 1B) and -5.2‰ at 3 cm at PS (Fig. 1F). At PS, TOC concentrations increase slightly with depth, with the mean content almost doubled compared to DS (Fig. 1C and G, Table S1). With respect to its stable carbon isotope composition, $\delta^{13}\text{C}$ -TOC increased slightly with depth at PS, from -28‰ in surficial sediments to -26‰ below 7 cm whereas $\delta^{13}\text{C}$ -TOC values remained relatively constant at DS throughout the sampled sediment column ($\sim -26\text{‰}$). The elemental C/N ratios in the sediments of DS show a very high variability with depth, and range from 6.7 to 16.8, with a mean value of 10.7 (Fig. 1D and Table S1), while the values at PS are lower and less variant along the sediment core (7.9 ± 0.3 , Fig. 1H).

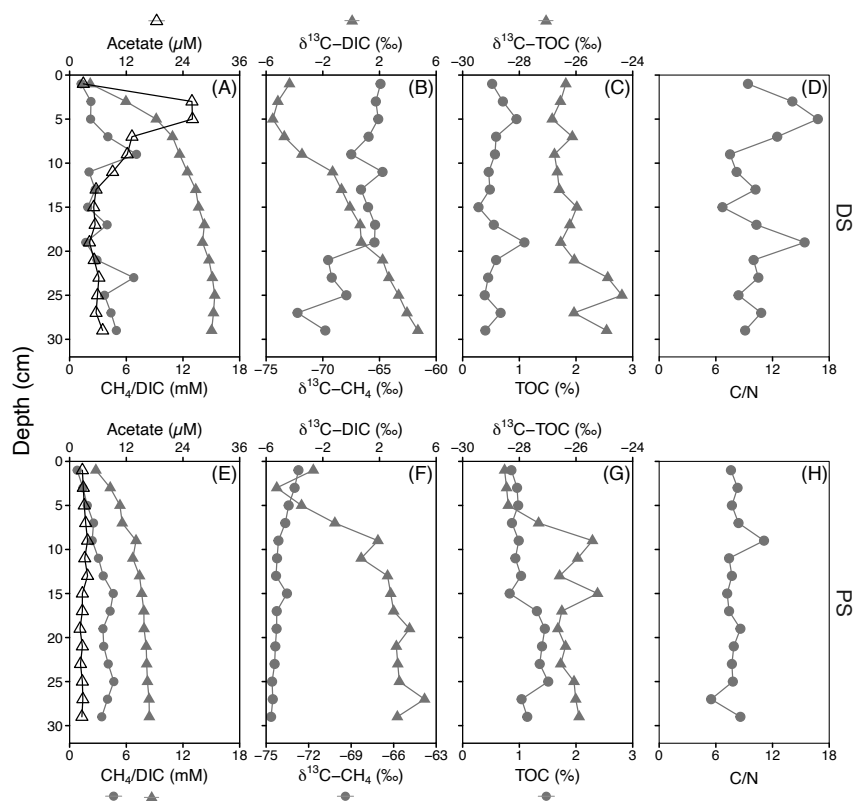


Figure 1. Sediment geochemistry as function of depth at a deltaic site (DS, A-D) and a profundal site (PS, E-H) in Lake Geneva. (A, E) Profiles of dissolved methane, dissolved inorganic carbon (DIC) and acetate concentrations. (B, F) Stable carbon isotopic signatures ($\delta^{13}\text{C}$) of CH_4 and DIC (in ‰ vs. V-PDB). (C, G) Concentrations of total organic carbon (TOC, % of dry weight) and its carbon isotopic composition (in ‰ vs. V-PDB). (D, H) Molar ratios of total organic carbon to total nitrogen (C/N).

3.2. Composition of sedimentary organic matter

To investigate the molecular composition of sedimentary organic matter at the two different sites, sediment samples were further analyzed using Py-GC/MS. We identified a total of 65 individual organic compounds (Table S2), which can be classified into the following compound groups: carbohydrates, N-compounds, *n*-alkenes, *n*-alkanes, phenols, lignin oligomers, and (poly)aromatics. Both carbohydrates and N-compounds were the most abundant organic compound groups among the pyrolysis products, with no statistical difference between DS and PS (Fig. 2 A and B). At both sites, the



carbohydrates consisted mainly of compounds such as butenal, methylfuraldehyde and
 furanone, and N-compounds were dominated by pyrrole, pyridine, methyl-pyrrole and
 methyl-pyridine (Table S2), which are indicative of degraded products of carbohydrates
 and proteins (Schellekens et al., 2009; Tolu et al., 2017). Most strikingly, sediments at
 DS displayed significantly higher relative abundances of lignin ($p < 0.05$) and phenols
 ($p < 0.01$) compared to profundal sediments (Fig. 3D and E). In addition, we observed
 significantly higher relative abundances of *n*-alkenes at PS (Fig. 3C). This group
 contains monounsaturated short-chain *n*-C₁₅ to *n*-C₁₈ (Table S2), which were the most
 abundant organic compounds among the *n*-alkenes.

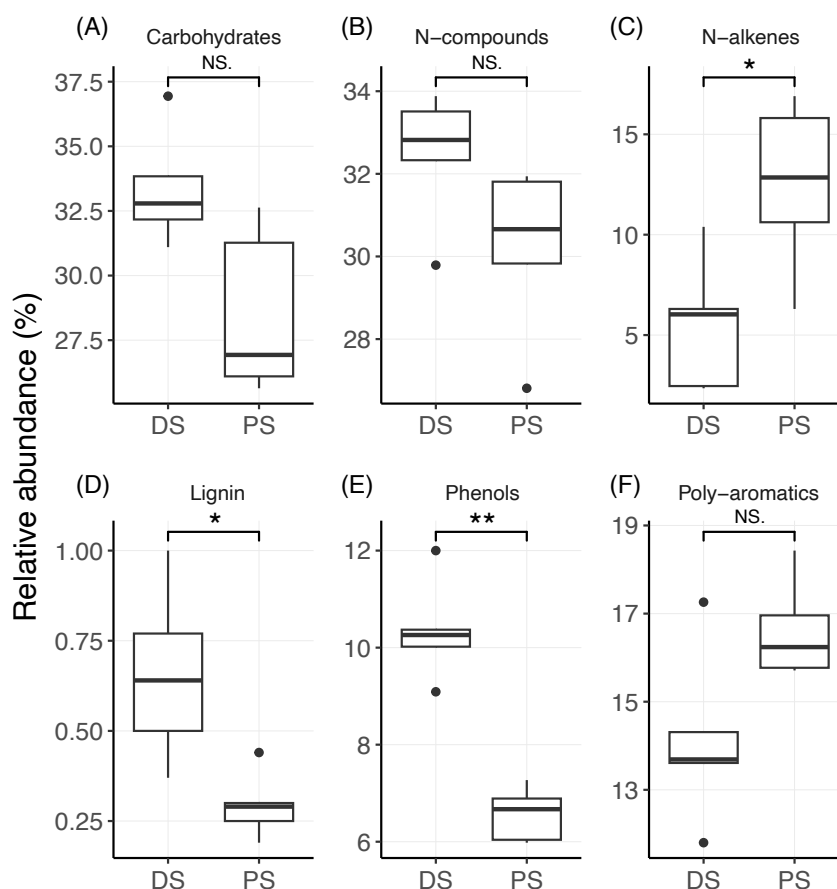


Figure 2. Relative abundances (in %) of different biochemical classes of organic
 compounds in sediments at the deltaic (DS) and profundal site (PS) of Lake Geneva.
 (A) Carbohydrates, (B) N-compounds, (C) N-alkenes, (D) Lignin, (E) Phenols and (F)



434 Poly-aromatics. Statistical differences of compound abundances between the two sites
 435 were determined with the Wilcoxon signed-rank test. Significance levels are: ** $p < 0.01$;
 436 * $p < 0.05$; NS. no significant differences between the two sites ($p > 0.05$).

437

438 **3.3. Lipid concentration, distribution, and stable carbon isotopic signature**

439 Typical lipid biomarkers derived from aquatic phytoplankton (e.g., short-chain
 440 fatty acids) and terrestrial plants (e.g., long-chain n-alkanes) were present in both
 441 profundal and deltaic sediments, yet concentrations of some of these biomarkers were
 442 strikingly different between the two sites, as well as between different depths within
 443 the same site (Fig. 3 and Table S3). Among the fatty acids, n -C_{16:0} was by far the most
 444 abundant in all measured samples, with a slight increase in $\delta^{13}\text{C}$ values with depth at
 445 both sites. At DS, the unsaturated fatty acids n -C_{16:1 ω 7} was the most abundant
 446 monounsaturated fatty acids with the highest concentration observed at 11cm. At PS,
 447 n -C_{16:1} (ω 7 and ω 5) and n -C_{18:1} (ω 9 and ω 7) decreased in concentration with depth and
 448 were two to four times more abundant in the upper sediment layers (0-2 cm, 4-6 and
 449 10-12 cm) than in the lower parts (18-20 and 28-30 cm). The short-chain fatty acids
 450 were generally depleted in ^{13}C , with stronger ^{13}C -depletions observed in surface
 451 sediments, particularly for the unsaturated fatty acids n -C_{16:1 ω 5} at PS.

452 In contrast to short-chain fatty acids, C_{24:0} was most abundant among the long-
 453 chain fatty acids (i.e., C_{24:0}, C_{26:0} and C_{28:0}), with relatively higher concentrations found
 454 in profundal sediments. Most strikingly, an apparent increase in the concentrations of
 455 these long-chain fatty acids was observed in the sediments of PS, with consistently high
 456 concentrations in the lower parts (10-30 cm). Meanwhile, the $\delta^{13}\text{C}$ values of these
 457 compounds decreased dramatically with depth. By comparison, concentrations of long-
 458 chain fatty acids at DS were variable at different sediment depths, but their $\delta^{13}\text{C}$ values
 459 remained relatively constant (e.g., C_{28:0}, Fig. 3B) and showed less variability with depth
 460 compared with PS (e.g., C_{24:0} and C_{26:0}). Although the concentrations of long-chain n-
 461 alkanes at DS were twice as high as those at PS, their $\delta^{13}\text{C}$ values (particularly for C₂₉,
 462 C₃₁ and C₃₃) were very similar at the two sites (Fig. 3B).

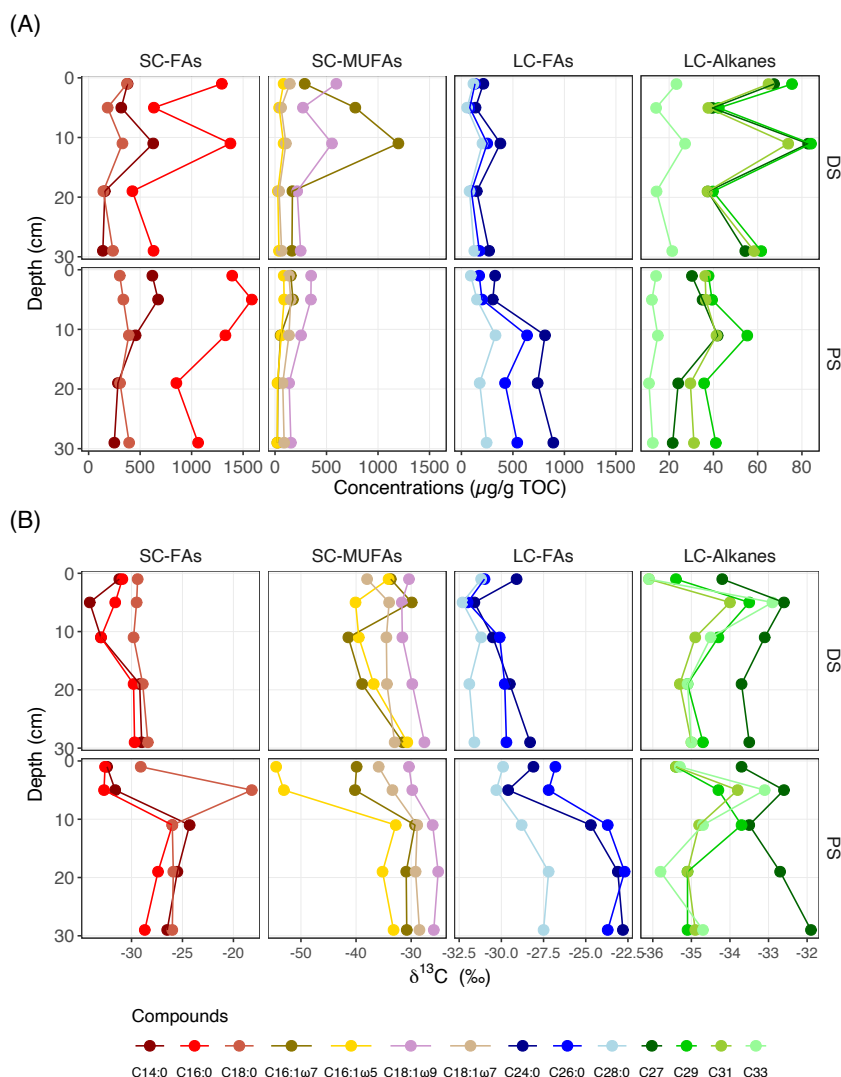
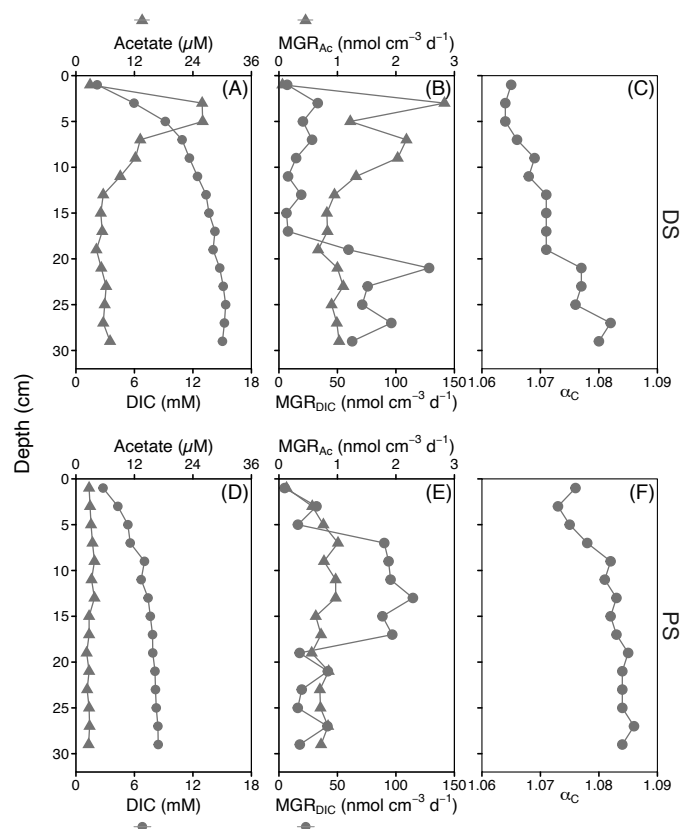


Figure 3. Vertical distribution of specific fatty acids and n-alkanes in deltaic (DS) and profundal (PS) sediments of Lake Geneva. (A) Concentrations (expressed as $\mu\text{g lipid g}^{-1} \text{ TOC}$), and (B) compound-specific $\delta^{13}\text{C}$ values (in ‰ vs. V-PDB). SC-FAs, short-chain fatty acids ($\text{C}_{14:0} + \text{C}_{16:0} + \text{C}_{18:0}$); SC-MUFAs, short-chain monounsaturated fatty acids ($\text{C}_{16:1}$ and $\text{C}_{18:1}$); LC-FAs, long-chain fatty acids ($\text{C}_{24:0} + \text{C}_{26:0} + \text{C}_{28:0}$); LC-Alkanes, long-chain n-alkanes ($\text{C}_{27} + \text{C}_{29} + \text{C}_{31} + \text{C}_{33}$).

3.4. Relative importance of methanogenic pathways



472 Methane production through CO₂ reduction (i.e., hydrogenotrophic
473 methanogenesis) was observed at both sites and at all depths. At the deltaic site, highest
474 activity of hydrogenotrophic methanogenesis was found at the lower part of the
475 sediment core (19-29 cm), while in the profundal sediment, maximum rates of
476 hydrogenotrophic methanogenesis were detected within the upper sediments at depths
477 between 7 and 17 cm (Fig. 4B and E, Table S1). In contrast, the rates of methane
478 production via acetate fermentation (i.e., acetoclastic methanogenesis) were very low,
479 with maxima of 2.8 and 1.0 nmol cm⁻³ d⁻¹ observed at 3 cm (PS) and 7 cm (DS),
480 respectively. The areal methanogenesis rates by CO₂ reduction within the top 30 cm, at
481 both sites, were two orders of magnitude higher than acetoclastic methanogenesis rates
482 (Table S1). Acetate oxidation activity was very low at both PS and DS, with the depth-
483 integrated (0-30 cm) rates of 0.1 and 0.2 mmol m⁻² d⁻¹, respectively (Table S1). At both
484 sites, the fractionation factor α_c , which is approximated based on the difference between
485 the measured $\delta^{13}\text{C-DIC}$ and $\delta^{13}\text{C-CH}_4$ values, increased with depth (Fig. 4F), ranging
486 from 1.064-1.071 (DS) and 1.073-1.084 (PS).
487



488
 489 Figure 4. Depth profiles of (A, D) porewater dissolved inorganic carbon (DIC) and
 490 acetate, (B, E) CO₂ reduction (MGR_{DIC}) and acetoclastic (MGR_{Ac}) methanogenesis
 491 rates, (C, F) apparent fractionation factor α_c in sediments of deltaic (DS) and profundal
 492 site (PS) in Lake Geneva. α_c is an approximation of the apparent C-isotope fractionation
 493 during methanogenesis, calculated from δ¹³C-CH₄ and δ¹³C-DIC values, where α_c =
 494 (1000 + δ¹³C-DIC)/(1000 + δ¹³C-CH₄). Values of α_c > 1.065 indicate predominance of
 495 CO₂ reduction over acetoclastic methanogenesis (Conrad, 2005b).

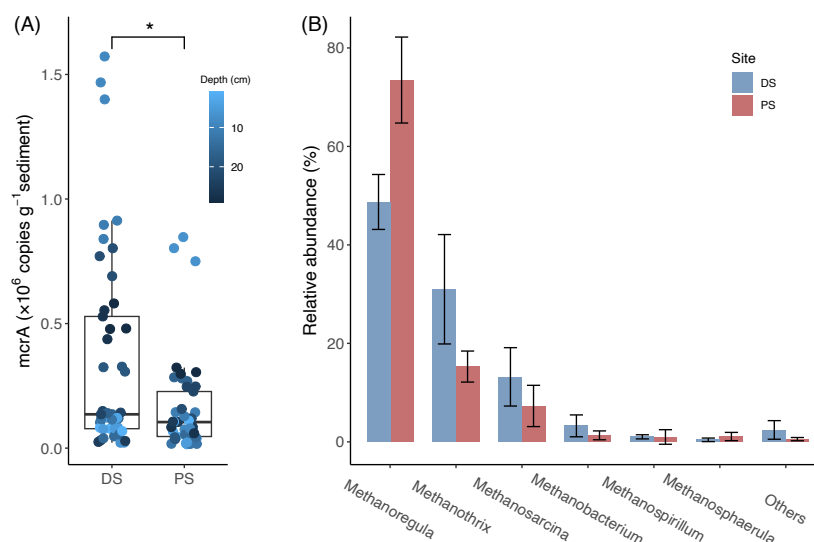
496

497 3.5. Abundance and diversity of methanogenic archaea

498 On average, gene copy numbers of the methyl coenzyme M reductase gene (*mcrA*)
 499 in the deltaic sediments of Lake Geneva were significantly higher than those in the
 500 profundal sediments ($p < 0.05$; Fig. 5A). At both sites, *Methanoregula* and
 501 *Methanotherix* dominated the methanogenic guild, followed by *Methanosarcina* and
 502 *Methanobacterium* (Fig. 5B). Within the methanogenic community, the mean relative



503 abundances of *Methanothrix* and *Methanosarcina* were both higher at DS than those at
 504 PS. By comparison, *Methanoregula* was the most abundant genus in the methanogenic
 505 community at PS. This matches recent studies on other lakes in Switzerland, in which
 506 *Methanoregula* was found to dominate methanogenic communities in the sediments
 507 (*Bartosiewicz et al., 2024; Meier et al., 2024*). Both *Methanoregula*, *Methanobacterium*
 508 and *Methanosphaerula* use H_2/CO_2 as the main substrates for methanogenesis (Oren,
 509 2014a). While *Methanothrix* have long been considered to use exclusively acetate as
 510 substrate for methanogenesis (Jetten et al., 1992; Smith and Ingram-Smith, 2007), there
 511 is now evidence that some species can also perform CO_2 reduction via direct
 512 interspecies electron transfer (DIET) (Rotaru et al., 2014; Zhou et al., 2023). Also,
 513 *Methanosarcina* can utilize a broader range of substrates, including CO_2 reduction with
 514 H_2 or via DIET, acetate, as well as some methylated compounds (Oren, 2014b).
 515



516
 517 Figure 5. Abundance and diversity of methanogens at the deltaic (DS) and the profundal
 518 site (PS) in Lake Geneva. (A) Absolute abundances of the *mcrA* gene encoding the α -
 519 subunit of the methyl-coenzyme M reductase. Statistical difference between the two
 520 sites was determined with the Wilcoxon signed-rank test and asterisk denotes
 521 significance level (*: $p < 0.05$). (B) Mean relative abundances of different methanogenic
 522 groups (% of the total methanogens). Data are based on read abundances of 16S rRNA
 523 gene sequences.
 524



525 **3.6. Correlation analysis between geochemical parameters, methane production** 526 **rates, and microbial communities**

527 The alpha diversity measures indicate that the community structure of
 528 microorganisms in the sediments at DS were more diverse than at PS (Fig. S2).
 529 Principal coordinate analysis (PCoA) revealed significantly different microbial
 530 community compositions at the two investigated sites, as indicated by the clear
 531 separation of the data by the first principal coordinates, explaining 50.8% and 44.5%
 532 of the observed variance for archaea and bacteria, respectively (Fig. S3). For both
 533 archaeal and bacterial communities, PCoA plots show a very close aggregation of the
 534 deep sediment samples at PS (17, 23 and 29 cm), indicating that their community
 535 structures are highly similar. Conversely, there is quite some variance among the
 536 samples at the more dynamic deltaic site DS, with its variable deposition history. The
 537 measured rates of both CO₂ reduction and acetoclastic methanogenesis tend to be higher
 538 in sediment samples harboring a more diverse microbial community (Fig. S4), but the
 539 relation is weak and particularly for acetoclastic methanogenesis not significant.
 540 Pearson correlation analysis between methane production rates and environmental
 541 parameters show that methane production rates from both MGR_{DIC} and MGR_{Ac} was
 542 positively but not significantly correlated with the concentration of short-chain n-
 543 alkanes (correlation coefficients of 0.46 and 0.51 for MGR_{DIC} and MGR_{Ac},
 544 respectively, Fig. S5). δ¹³C-CH₄ values showed a positive correlation with the
 545 abundance of carbohydrates, lignin, and long-chain n-alkanes, and significant negative
 546 correlation with the abundance of long-chain fatty acids and total organic carbon. C/N
 547 ratios were negatively correlated with the concentrations of both short-chain and long-
 548 chain fatty acids (Fig. S5).

549

550 **4. Discussion**

551 Our results indicate a dominance of methane production by CO₂ reduction in both
 552 profundal and deltaic sediments of Lake Geneva. This inference is supported by
 553 radiotracer measurements, the observed apparent fractionation factors, and
 554 methanogenic community analyses, which revealed members of CO₂-reducing
 555 *Methanoregula* as the dominant group of methanogens. Thus, CO₂ reduction was
 556 observed as the primary MGR process both in sediments at PS, which predominantly
 557 contained diagenetically altered phytoplankton-derived OC, and sediments at DS



558 characterized by variable sources of aquatic and terrestrial OC. We conclude, therefore,
559 that the dominant pathway of methanogenesis does not primarily depend on the
560 chemical composition of sedimentary organic matter. Other factors that affect
561 production rates of different electron donors (e.g., H₂, acetate) could play a more
562 important role, and will be discussed below.

563

564 **4.1. Difference in organic carbon sources and diagenetic alteration**

565 The deltaic sediments in this study displayed a strikingly large range of C/N ratios
566 (6.7-16.8), whereas C/N ratios of profundal samples remained relatively constant
567 throughout the sediment core (7.9 ± 0.3). Fresh organic matter from lacustrine
568 phytoplankton, which is protein- rich (Parsons et al., 1961), typically has low C/N ratios
569 of 6-9 (Meyers and Ishiwatari, 1993). In contrast, bulk sediment containing large
570 portions of terrestrial vascular plants often displays much higher C/N ratios, sometimes
571 at least three times greater, due to its high content of high-carbon structural components
572 and refractory organics such as lignin (Hedges et al., 1986). A comparison of carbon
573 isotope and bulk C/N values to data from previous studies (Lamb et al., 2006)
574 confirmed the presence of both aquatic and terrestrial sources in the deltaic sediments,
575 and the dominance of organic matter of autochthonous origin (e.g., algal biomass) at
576 PS (Fig. 6). At DS, variable microbial community structures and significant changes in
577 C/N ratios with depth reflect a highly variable depositional history, indicating differing
578 origins of sedimentary organic matter. Specifically, peak C/N ratios of 16.8 at 5 cm and
579 15.4 at 19 cm were likely derived from terrestrial organic matter in these intercalated
580 layers, while relatively lower ratios (~ 10) at other depths suggest a mixture of aquatic
581 and terrestrial sources. Even lower values (~ 7) in some deltaic sediment layers may
582 indicate predominantly autochthonous deposition of phytoplankton particles.

583

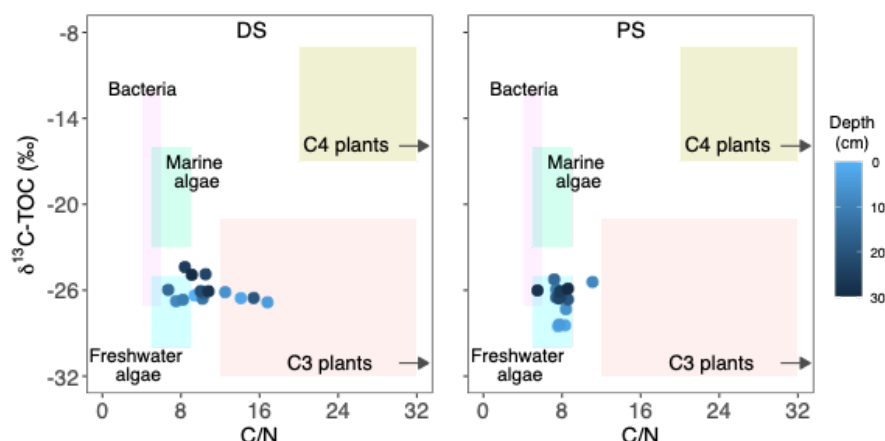


Figure 6. Comparison of $\delta^{13}\text{C}$ and bulk C/N values of Lake Geneva sediments from the deltaic (DS, left) and profundal site (PS, right) to elemental and isotopic indicators of bulk organic matter produced by bacteria, marine and freshwater algae, as well as terrestrial C3 and C4 plants (Lamb et al., 2006).

Indeed, at both sites, sediments contained OC from aquatic biomass, as verified by the short-chain fatty acids, indicative of freshwater algae (Cranwell, 1976), and/or in situ production by bacteria (Volkman et al., 1998). However, contrary to the findings from the combined carbon isotope and bulk C/N ratios, both lignin/phenols (Fig. 2) and long-chain n-alkanes (Fig. 3A) derived from terrestrial plants were detected in profundal sediments, although the concentrations of these compounds were lower at PS than at DS. Long-chain fatty acids (i.e., $\text{C}_{24:0}$ and $\text{C}_{26:0}$), which are typically assumed to originate from terrestrial plant waxes (Cranwell, 1974), make up a proportionally more important fraction of lipids in deeper sediment layers, particularly below 5 cm depth. However, the distinct carbon isotope compositions of these long-chain fatty acids between the two sites (Fig. 3B and Table S3, $\delta^{13}\text{C}$ on average $\sim 7\text{‰}$ lower at DS than at PS) suggest different OC sources.

Indeed, Chikaraishi et al. (2004) reported that long-chain fatty acids (i.e., $\text{C}_{24:0}$ and $\text{C}_{26:0}$) have $\delta^{13}\text{C}$ values of $-36.3 \pm 2.6\text{‰}$ for a variety of terrestrial vascular plants, whereas the $\delta^{13}\text{C}$ for aquatic plants is significantly less negative ($-25.5 \pm 0.9\text{‰}$). At PS, $\delta^{13}\text{C}$ values for $\text{C}_{24:0}$ and $\text{C}_{26:0}$ fatty acids (below 5 cm depth) were close to those indicative of freshwater aquatic plants (Chikaraishi et al., 2004). Previous studies have shown that both aquatic macrophytes and microalgae may represent potential sources



608 of long-chain fatty acids (Ficken et al., 2000; Volkman et al., 1998). However, it seems
 609 somewhat contradictory to conclude that long-chain fatty acids were primarily derived
 610 from aquatic vascular plants, simply because the observed C/N ratios at PS were too
 611 low. Indeed, microalgae such as diatoms were estimated to contribute from 30-80% of
 612 the C_{24:0} to C_{28:0} fatty acid pool in intertidal sandy sediment (Volkman et al., 1980).
 613 Thus, the long-chain fatty acids observed in the profundal sediments may also have
 614 been derived from microalgae (Volkman et al., 1998). This, in turn, could explain why
 615 TOC was more depleted in ¹³C in the surface sediments at PS, which does not
 616 necessarily indicate the origins of terrestrial plants (Cloern et al., 2002).

617 The carbon isotopic composition of long-chain n-alkanes (i.e., C₂₇₋₃₁),
 618 characteristic for land-derived organic matter (Chikaraishi et al., 2004), was almost
 619 identical between PS and DS (Fig. 3B, ranging from -35‰ to -33‰), suggesting a
 620 similar terrestrial source. At DS, if long-chain n-alkanes and long-chain fatty acids were
 621 derived from the same terrestrial source, they should have similar C-isotopic values.
 622 However, the slightly lower ^δ¹³C values of long-chain fatty acids at DS (on average, -
 623 30‰) imply a mixture of both aquatic and terrestrial sources, which is consistent with
 624 the C/N ratios observed at this site.

625 Turning to other OM biomarkers, phytol concentrations were considerably higher
 626 at PS (with no clear depth trend) compared to DS, whereas no clear difference in
 627 cholesterol concentrations was observed between the sites (with depth-dependent
 628 concentration decrease at both sites). For brassicasterol, there seems to be a clear depth-
 629 related decrease at both sites, with slightly higher concentrations in surface sediments
 630 (0-2 and 4-6 cm) at PS compared to DS. Phytol, a side chain of chlorophyll, can
 631 originate from both phytoplankton and terrestrial plants (Shi et al., 2001). Due to its
 632 rapid degradation under intense-light and oxic conditions in terrestrial environments,
 633 terrestrially derived phytol (or chlorophyll) is generally of minor importance in aquatic
 634 sediments (Meyers and Takeuchi, 1981), so it can be assumed that most of the
 635 sedimentary phytol is derived from aquatic sources (Ladd et al., 2018). As for
 636 cholesterol and brassicasterol (Table S3), the former can originate from both
 637 zooplankton and phytoplankton (Bechtel and Schubert, 2009), while the latter is a lipid
 638 biomarker mainly derived from phytoplankton in aquatic sediments (Volkman, 1986).
 639 Hence, based on at least two of the biomarkers presented here, we have putative
 640 evidence for a shift towards more autochthonous OM at the profundal site, as could be
 641 expected.



642

643 **4.2. Methanogenesis is mainly driven by CO₂ reduction**

644 Our rate measurements using trace ¹⁴C-labelled substrates clearly showed that CO₂
 645 reduction played a dominant role in methane formation in both the PS and DS
 646 sediments, compared to acetoclastic methanogenesis. As we did not measure rates of
 647 methylotrophic methanogenesis, we are unable to determine the relative importance of
 648 this pathway. However, since we neither detected common methylated compounds
 649 such as methanol in the sediment porewater, nor methanogens that exclusively perform
 650 methylotrophic methanogenesis at any of the studied sites, we argue that this pathway
 651 is likely of a minor importance with regards to its the contribution to the overall
 652 methane production at these sites. Indeed, H₂/CO₂ and acetate are usually the main
 653 substrates in freshwater environments (Lyu et al., 2018), and to date, no direct evidence
 654 for the occurrence of methylotrophic methanogenesis has been documented for lake
 655 sediments. Methylotrophic methanogenesis has been shown to be an important pathway
 656 mainly in specific marine systems, where methanogens can utilize methylated
 657 compounds (e.g., methanol and trimethylamine) as non-competitive substrates for
 658 methane production (Xiao et al., 2018; Xu et al., 2021; Zhuang et al., 2018).

659 The finding that CO₂ reduction pathway dominated methane production
 660 throughout the sediment cores at both sites was further supported by the observed
 661 apparent fractionation factor α_c (DS: 1.071 ± 0.001 and PS: 1.081 ± 0.001 ; Fig. 4C, F
 662 and Table S1) (Conrad, 2005). Rates for CO₂ reduction in Lake Geneva were similar at
 663 the two studied sites, but were much higher than those previously reported in other
 664 lakes at similar depths (Kuivila et al., 1989). The observed low rates for acetoclastic
 665 methanogenesis on the other hand were comparable to those in other lake sediments
 666 (Kuivila et al., 1989; Schulz and Conrad, 1996). Methane production via acetate
 667 fermentation was traditionally believed to play a more important role than via CO₂
 668 reduction in lake sediments (Whiticar, 1999; Whiticar et al., 1986). However, more
 669 recent evidence seems to contradict this paradigm, demonstrating that
 670 hydrogenotrophic methanogenesis can indeed be a much more significant methane-
 671 producing biogeochemical pathway than acetoclastic methanogenesis (Blair et al.,
 672 2018; Conrad et al., 2011; Meier et al., 2024). The predominance of methane formation
 673 via CO₂ reduction over acetoclastic methanogenesis is an important finding, which, in
 674 Lake Geneva, appears to apply to sediments across different sedimentary depositional
 675 regimes.



At both sites, *Methanoregula* was the most abundant methanogenic genus, particularly in deep sediments where the highest CO₂ reduction rates were observed. This genus, commonly found in freshwater lakes (Bartosiewicz et al., 2024; Berberich et al., 2020; Meier et al., 2024), is known to perform hydrogenotrophic methanogenesis. *Methanothrix*, the second most abundant methanogen, primarily performs acetoclastic methanogenesis, although some species within this cluster can also produce methane via CO₂ reduction (Rotaru et al., 2014). At PS, *Methanoregula* dominated at all investigated depths, in accordance with high rates of autotrophic methanogenesis. While acetoclastic methanogenesis played only a minor role in total methane production, higher rates were observed for deltaic sediments, with lower apparent fractionation factor. This observation is consistent with higher concentrations of acetate and a higher relative abundance of acetate-consuming *Methanothrix*, suggesting that the pathway of acetoclastic methanogenesis was influenced by both the availability of acetate and the functional methanogenic population.

Although overall methane production rates were similar at both sites, the qPCR data in hand indicated that bulk methane production was not primarily/directly controlled by (i.e., proportional to) the cell abundance of methanogens. Instead, it was likely regulated by other environmental factors, such as limited substrate availability/supply (i.e., H₂ and acetate), stemming from rates of hydrolysis (Kristensen et al., 1995) and/or fermentation rates (Valentine et al., 1994) within the sediments. Methanogens depend on syntrophic and other heterotrophic bacteria, which may significantly influence methane production rates (Beulig et al., 2018; Liu and Whitman, 2008).

In Lake Geneva sediments, rates of both CO₂ reduction and acetoclastic methanogenesis increased with microbial Shannon diversity. More diverse microbial communities tend to possess more diverse organic matter degradation capacities, resulting in higher production of acetate and H₂/CO₂, which in turn promotes overall methane production (Conrad, 2020). However, our microbial abundance and diversity data were insufficient to fully characterize the carbon metabolism of microorganisms involved in H₂ and acetate production, which could directly impact CO₂ reduction and acetoclastic methanogenesis and potentially explain the observed methane production differences. The very low acetate oxidation rates at both sites suggest that differences in methane generation via MGR_{DIC} versus MGR_{Ac} may be attributed to the relative availability of methane precursors available (i.e., H₂/CO₂ versus acetate) (Capone and



710 Kiene, 1988). The acetate concentrations were low (below 26 μM) at both sites, but
 711 well within the range of what has been measured in profundal sediment of Lake
 712 Constance, where acetoclastic methanogenesis was dominant (Schulz and Conrad,
 713 1996). Hence, the consistently low rates of acetoclastic methanogenesis throughout the
 714 sediment cores at both sites likely resulted from low turnover rates of acetate during
 715 organic matter degradation.

716

717 **4.3. Effect of organic carbon characteristics on methanogenesis**

718 Despite the differences in OC sources and quality between the two sites, the overall
 719 methane production rates were comparable (Fig. 4B, E and Table S1). However, the
 720 sedimentary zones of maximum methane production and the depth-dependent rates of
 721 both metabolic modes of methanogenesis varied. This likely reflects differences in OC
 722 quality and degradation pathways, which influence the balance between
 723 remineralization to H_2/CO_2 versus acetate (Conrad, 2020), resulting in spatial
 724 variability in sedimentary methane production.

725 Potential methane production rates have been shown to correlate positively with
 726 the quantity of sediment organic matter (Berberich et al., 2020). However, at both the
 727 DS and PS in Lake Geneva, the sediment layers of maximum rates of CO_2 reduction
 728 did not coincide with higher TOC contents. Instead, combined rate and isotopic
 729 measurements revealed that methanogenesis rates via CO_2 reduction corresponded to
 730 less ^{13}C -depleted bulk organic carbon (Fig. 1 and 4). This suggests that the source and
 731 microbial decomposition of organic matter, rather than its quantity, primarily
 732 influenced the methanogenic activity via the CO_2 -reduction pathway.

733 Methane production rates in lake sediments are generally low across various
 734 latitudes but can increase significantly with the addition of fresh organic carbon
 735 (Bartosiewicz et al., 2024; Schwarz et al., 2008; West et al., 2012). Indeed, high lipid
 736 contents in phytoplankton biomass have been shown to enhance methane production in
 737 both engineered systems and lake sediments (West et al., 2015; Zhao et al., 2014).
 738 Additionally, existing evidence suggest that terrestrial OC can stimulate methane
 739 ebullition in reservoirs (DelSontro et al., 2011; Sobek et al., 2012). Our findings from
 740 rate measurement and organic carbon composition agree with earlier studies, indicating
 741 that both aquatic and terrestrial OC can significantly contribute to methane production
 742 (Berberich et al., 2020; Grasset et al., 2018). It has also been suggested that the
 743 availability of easily degradable organic matter controls both methanogenic pathways



744 and methanogenic archaeal communities (Liu et al., 2017). However, the influence of
 745 organic matter source or composition on the relative importance of methane production
 746 pathways and their corresponding rates remains poorly constrained and has rarely been
 747 explored. Within the zone of high hydrogenotrophic activity at PS, TOC became less
 748 depleted in ^{13}C , a trend also observed, though less pronounced, in the deltaic sediments.
 749 The $\delta^{13}\text{C}$ shift of TOC within the most active zone at PS likely resulted from the
 750 selective loss of isotopically light OM fractions (Lehmann et al., 2002b; Meyers, 1994),
 751 or the changes in organic matter sources, as suggested by variations in both short-chain
 752 and long-chain fatty acids indicative of autochthonous origins.

753 Contrary to previous studies demonstrating that algal deposition stimulated the
 754 activity of acetoclastic methanogens (Schulz and Conrad, 1995; Schwarz et al., 2008),
 755 our results revealed higher acetate concentrations in tandem with higher acetoclastic
 756 methanogenesis occurring in surface sediments of deltaic site, where high C/N ratios
 757 indicated terrestrial inputs. This suggests that allochthonous OC may play a role in
 758 acetate production and acetoclastic methanogenesis. However, the apparently much
 759 lower overall acetoclastic rates compared CO_2 reduction were likely due to the active
 760 acetate consumption via syntrophic oxidation (Conrad et al., 2020). At PS,
 761 autochthonous organic matter was the dominant OC source to the sediments, and the
 762 CH_4 produced likely resulted from the decomposition of buried algal detritus (Fig. 6).
 763 This interpretation is also supported by the 2-fold higher brassicasterol, the 3-fold
 764 higher phytol, and 3-4-fold higher long chain fatty acids concentrations (with elevated
 765 $\delta^{13}\text{C}$ values) at PS compared to DS. These biomarkers, in combination with lower C/N
 766 ratios, are indicative of algal material as the dominant organic contributor to early
 767 diagenetic methane production.

768 While the dominant sedimentary organic matter source (i.e., the partitioning
 769 between autochthonous versus allochthonous OM inputs to the sediments) varied
 770 between the two studied sites, the similar overall methane production rates imply that
 771 methanogenesis occurred ubiquitously in these lacustrine sediments, independent of the
 772 OC sources, their apparent susceptibility to organic matter degradation, and/or their
 773 overall diagenetic state. This finding aligns with a recent study across the river/deltaic-
 774 pelagic continuum in a reservoir system in southwest Ohio (Berberich et al., 2020), and
 775 holds important implications for understanding the lacustrine methane cycle. On the
 776 one hand, eutrophication in lakes and other aquatic systems often increases the supply
 777 of autochthonous organic carbon, thereby enhancing methanogenesis and leading to



778 increased methane emissions (Davidson et al., 2018). On the other hand, the potential
 779 of terrestrial organic matter to contribute to lacustrine methane production can be
 780 significantly impacted by anthropogenic activities, such as dam construction (Li et al.,
 781 2023), or as a result of deforestation and soil erosion, which alter sediment inputs into
 782 the lake (Bélanger et al., 2017). Difference in the source and lability of organic carbon
 783 in the lacustrine organic matter pool may affect sediment methane production in distinct
 784 ways (Grasset et al., 2018; Stibal et al., 2012). Our study demonstrates that diverse OC
 785 sources and varying diagenetic states in both profundal and deltaic sediments support
 786 substantial rates of methane formation through CO₂ reduction. However, identifying
 787 the exact fractions of organic matter that were degraded and fueled methane production
 788 remains challenging. While acetoclastic methanogenesis appears to be relevant to the
 789 break-down and decomposition of terrestrial organic matter that favors acetate
 790 production and accumulation in deltaic sediments, the sources of organic carbon driving
 791 the more dominant CO₂-reducing methanogenesis in the studied sediments remains
 792 unclear. The key environmental factors controlling the organic matter degradation in
 793 methanogenic sediments remain unresolved and require further investigation.
 794 Understanding these mechanisms is essential for predicting how changes in organic
 795 carbon inputs and sediment dynamics may influence methane production and emissions
 796 from lacustrine environments.

797

798 **5. Conclusions**

799 Our study demonstrates that both profundal and deltaic sediments of Lake Geneva
 800 are significant sources of methane, despite clear differences in origins and compositions
 801 of organic matter. The profundal site is dominated by aquatic OM, while the deltaic site
 802 features a more variable mix of OM sources, including substantial terrestrial
 803 contributions at certain depths. Methane production at both sites is overwhelmingly
 804 driven by CO₂ reduction, which accounted for over 95% of total methane production
 805 and was most probably mediated by *Methanoregula*. While phylogenetic data suggest
 806 a link between methanogen communities and methanogenetic pathways, the broader
 807 microbial community dynamics, particularly those involved in H₂ and acetate
 808 production, remain insufficiently understood.

809 At the profundal site, methane production is mainly associated with the
 810 decomposition of aquatic organic matter, as terrestrial OC is less abundant. At the



811 deltaic site, acetoclastic methanogenesis appears linked to the higher terrestrial organic
812 matter inputs. Nevertheless, the overall dominance of methanogenesis via CO₂
813 reduction at both sites suggests that depositional regime, as well as OM source and
814 composition are not the primary determinants of the prevailing methane producing
815 pathway. Instead, factors such as the metabolic interactions within microbial
816 communities (e.g., with syntrophic partner organisms), particularly the balance of H₂
817 and acetate production, may play a larger role. Future research should focus on
818 unraveling these interactions to better predict if, and how, changes in OM inputs and
819 sediment dynamics may impact methane emissions from lacustrine environments.
820



821 **Data availability statement**

822 Raw reads of the 16S rRNA sequencing data are available on NCBI GenBank with
823 BioProject ID PRJNA736863, under accession number SRR14794332- SRR14794339.
824

825 **Author contributions**

826 CJS, GS and MAL conceived the research. CJS acquired funding for this study.
827 GS performed field work, lab experiments and data analyses. JT assisted with
828 Pyrolysis-GC data analysis. CG and MAL measured porewater volatile fatty acids and
829 analyzed the data. JZ and MFL helped with rate measurements and molecular analyses.
830 GS wrote the original draft of the manuscript. All authors revised and approved the
831 submitted version.
832

833 **Acknowledgements**

834 This research was supported by Eawag internal funds. We thank Alois Zwyssig,
835 Sandra Schmid and Cameron M. Callbeck for assistance with field sample collection.
836 We also thank Serge Robert for laboratory assistance including lipid sample preparation
837 and laboratory analyses and for his help in elemental analysis of samples. Patrick
838 Kathriner is acknowledged for laboratory support. We are also grateful to Thomas
839 Kuhn at the University of Basel for laboratory support with the radioisotope
840 measurements.
841

842 **Competing interests**

843 At least one of the (co-)authors is a member of the editorial board of
844 Biogeosciences.
845



846 **References**

- 847 Bartosiewicz, M., Przytulska, A., Birkholz, A., Zopfi, J., and Lehmann, M. F.:
 848 Controls and significance of priming effects in lake sediments, *Glob Chang Biol*,
 849 30, 1–13, <https://doi.org/10.1111/gcb.17076>, 2024.
 850 Bastviken, D., Tranvik, L. J., Downing, J. A., Crill, P. M., and Enrich-Prast, A.:
 851 Freshwater Methane Emissions Offset the Continental Carbon Sink, *Science*
 852 (1979), 331, 50–50, <https://doi.org/10.1126/science.1196808>, 2011.
 853 Bechtel, A. and Schubert, C. J.: A biogeochemical study of sediments from the
 854 eutrophic Lake Lugano and the oligotrophic Lake Brienz, Switzerland, *Org*
 855 *Geochem*, 40, 1100–1114, <https://doi.org/10.1016/j.orggeochem.2009.06.009>,
 856 2009.
 857 Bélanger, É., Lucotte, M., Moingt, M., Paquet, S., Oestreicher, J., and Rozon, C.:
 858 Altered nature of terrestrial organic matter transferred to aquatic systems
 859 following deforestation in the Amazon, *Applied Geochemistry*, 87, 136–145,
 860 <https://doi.org/10.1016/j.apgeochem.2017.10.016>, 2017.
 861 Berberich, M. E., Beaulieu, J. J., Hamilton, T. L., Waldo, S., and Buffam, I.: Spatial
 862 variability of sediment methane production and methanogen communities
 863 within a eutrophic reservoir: Importance of organic matter source and quantity,
 864 *Limnol Oceanogr*, 65, 1336–1358, <https://doi.org/10.1002/lno.11392>, 2020.
 865 Beulig, F., Røy, H., Glombitza, C., and Jørgensen, B. B.: Control on rate and
 866 pathway of anaerobic organic carbon degradation in the seabed, *Proc Natl Acad*
 867 *Sci USA*, 115, 367–372, <https://doi.org/10.1073/pnas.1715789115>, 2018.
 868 Blair, N. E., Leithold, E. L., Thanos Papanicolaou, A. N., Wilson, C. G., Keefer, L.,
 869 Kirton, E., Vinson, D., Schnoebelen, D., Rhoads, B., Yu, M., and Lewis, Q.: The C-
 870 biogeochemistry of a Midwestern USA agricultural impoundment in context:
 871 Lake Decatur in the intensively managed landscape critical zone observatory,
 872 *Biogeochemistry*, 138, 171–195, <https://doi.org/10.1007/s10533-018-0439-9>,
 873 2018.
 874 Burrus, D., Thomas, R. L., Dominik, J., and Vernet, J.-P.: Recovery and
 875 concentration of suspended solids in the upper rhone river by continuous flow
 876 centrifugation, *Hydrol Process*, 3, 65–74,
 877 <https://doi.org/10.1002/hyp.3360030107>, 1989.
 878 Capone, D. G. and Kiene, R. P.: Comparison of microbial dynamics in marine and
 879 freshwater sediments: Contrasts in anaerobic carbon catabolism, *Limnol*
 880 *Oceanogr*, 33, 725–749, <https://doi.org/10.4319/lo.1988.33.4part2.0725>, 1988.
 881 Chikaraishi, Y., Naraoka, H., and Poulson, S. R.: Hydrogen and carbon isotopic
 882 fractionations of lipid biosynthesis among terrestrial (C3, C4 and CAM) and
 883 aquatic plants, *Phytochemistry*, 65, 1369–1381,
 884 <https://doi.org/10.1016/j.phytochem.2004.03.036>, 2004.
 885 Cloern, J. E., Canuel, E. A., and Harris, D.: Stable carbon and nitrogen isotope
 886 composition of aquatic and terrestrial plants of the San Francisco Bay estuarine
 887 system, *Limnol Oceanogr*, 47, 713–729,
 888 <https://doi.org/10.4319/lo.2002.47.3.0713>, 2002.
 889 Conrad, R.: Quantification of methanogenic pathways using stable carbon
 890 isotopic signatures: a review and a proposal, *Org Geochem*, 36, 739–752,
 891 <https://doi.org/10.1016/j.orggeochem.2004.09.006>, 2005.
 892 Conrad, R.: Importance of hydrogenotrophic, acetoclastic and methylotrophic
 893 methanogenesis for methane production in terrestrial, aquatic and other anoxic



894 environments: A mini review, *Pedosphere*, 30, 25–39,
 895 [https://doi.org/10.1016/S1002-0160\(18\)60052-9](https://doi.org/10.1016/S1002-0160(18)60052-9), 2020.
 896 Conrad, R., Noll, M., Claus, P., Klose, M., Bastos, W. R., and Enrich-Prast, A.: Stable
 897 carbon isotope discrimination and microbiology of methane formation in
 898 tropical anoxic lake sediments, *Biogeosciences*, 8, 795–814,
 899 <https://doi.org/10.5194/bg-8-795-2011>, 2011.
 900 Conrad, R., Klose, M., and Enrich-Prast, A.: Acetate turnover and methanogenic
 901 pathways in Amazonian lake sediments, *Biogeosciences*, 17, 1063–1069,
 902 <https://doi.org/10.5194/bg-17-1063-2020>, 2020.
 903 Cranwell, P. A.: Monocarboxylic acids in lake sediments: Indicators, derived from
 904 terrestrial and aquatic biota, of paleoenvironmental trophic levels, *Chem Geol*,
 905 14, 1–14, [https://doi.org/10.1016/0009-2541\(74\)90092-8](https://doi.org/10.1016/0009-2541(74)90092-8), 1974.
 906 Cranwell, P. A.: Decomposition of aquatic biota and sediment formation: organic
 907 compounds in detritus resulting from microbial attack on the alga *Ceratium*
 908 *hirundinella*, *Freshw Biol*, 6, 41–48, <https://doi.org/10.1111/j.1365-2427.1976.tb01589.x>, 1976.
 909 Dai, J., Sun, M.-Y., Culp, R. A., and Noakes, J. E.: Changes in chemical and isotopic
 910 signatures of plant materials during degradation: Implication for assessing
 911 various organic inputs in estuarine systems, *Geophys Res Lett*, 32, L13608,
 912 <https://doi.org/10.1029/2005GL023133>, 2005.
 913 Davidson, T. A., Audet, J., Jeppesen, E., Landkildehus, F., Lauridsen, T. L.,
 914 Søndergaard, M., and Syväranta, J.: Synergy between nutrients and warming
 915 enhances methane ebullition from experimental lakes, *Nat Clim Chang*, 8, 156–
 916 160, <https://doi.org/10.1038/s41558-017-0063-z>, 2018.
 917 Dean, W. E. and Gorham, E.: Magnitude and significance of carbon burial in lakes,
 918 reservoirs, and peatlands, *Geology*, 26, 535, <https://doi.org/10.3133/fs05899>,
 919 1998.
 920 DelSontro, T., Kunz, M. J., Kempter, T., Wüest, A., Wehrli, B., and Senn, D. B.:
 921 Spatial Heterogeneity of Methane Ebullition in a Large Tropical Reservoir,
 922 *Environ Sci Technol*, 45, 9866–9873, <https://doi.org/10.1021/es2005545>, 2011.
 923 Demirel, B. and Scherer, P.: The roles of acetotrophic and hydrogenotrophic
 924 methanogens during anaerobic conversion of biomass to methane: a review, *Rev*
 925 *Environ Sci Biotechnol*, 7, 173–190, [https://doi.org/10.1007/s11157-008-9131-](https://doi.org/10.1007/s11157-008-9131-1)
 926 1, 2008.
 927 Downing, J. A., Prairie, Y. T., Cole, J. J., Duarte, C. M., Tranvik, L. J., Striegl, R. G.,
 928 McDowell, W. H., Kortelainen, P., Caraco, N. F., Melack, J. M., and Middelburg, J. J.:
 929 The global abundance and size distribution of lakes, ponds, and impoundments,
 930 *Limnol Oceanogr*, 51, 2388–2397, <https://doi.org/10.4319/lo.2006.51.5.2388>,
 931 2006.
 932 Eglinton, G. and Hamilton, R. J.: Leaf epicuticular waxes, *Science* (1979), 156,
 933 1322–1335, <https://doi.org/10.1126/science.156.3780.1322>, 1967.
 934 Ficken, K. J., Li, B., Swain, D. L., and Eglinton, G.: An n-alkane proxy for the
 935 sedimentary input of submerged/floating freshwater aquatic macrophytes, *Org*
 936 *Geochem*, 31, 745–749, [https://doi.org/10.1016/S0146-6380\(00\)00081-4](https://doi.org/10.1016/S0146-6380(00)00081-4),
 937 2000.
 938 Gallina, N., Beniston, M., and Jacquet, S.: Estimating future cyanobacterial
 939 occurrence and importance in lakes: a case study with *Planktothrix rubescens* in
 940 Lake Geneva, *Aquat Sci*, 79, 249–263, [https://doi.org/10.1007/s00027-016-](https://doi.org/10.1007/s00027-016-0494-z)
 941 0494-z, 2017.



- 943 Glombitza, C., Pedersen, J., Røy, H., and Jørgensen, B. B.: Direct analysis of volatile
 944 fatty acids in marine sediment porewater by two-dimensional ion
 945 chromatography-mass spectrometry, *Limnol Oceanogr Methods*, 12, 455–468,
 946 <https://doi.org/10.4319/lom.2014.12.455>, 2014.
- 947 Grasset, C., Mendonça, R., Villamor Saucedo, G., Bastviken, D., Roland, F., and
 948 Sobek, S.: Large but variable methane production in anoxic freshwater sediment
 949 upon addition of allochthonous and autochthonous organic matter, *Limnol*
 950 *Oceanogr*, 63, 1488–1501, <https://doi.org/10.1002/lno.10786>, 2018.
- 951 Han, X., Schubert, C. J., Fiskal, A., Dubois, N., and Lever, M. A.: Eutrophication as a
 952 driver of microbial community structure in lake sediments, *Environ Microbiol*,
 953 22, 3446–3462, <https://doi.org/10.1111/1462-2920.15115>, 2020.
- 954 Han, X., Tolu, J., Deng, L., Fiskal, A., Schubert, C. J., Winkel, L. H. E., and Lever, M.
 955 A.: Long-term preservation of biomolecules in lake sediments: potential
 956 importance of physical shielding by recalcitrant cell walls, *PNAS Nexus*, 1,
 957 <https://doi.org/10.1093/pnasnexus/pgac076>, 2022.
- 958 Hansen, L. K., Jakobsen, R., and Postma, D.: Methanogenesis in a shallow sandy
 959 aquifer, Rømø, Denmark, *Geochim Cosmochim Acta*, 65, 2925–2935,
 960 [https://doi.org/10.1016/S0016-7037\(01\)00653-6](https://doi.org/10.1016/S0016-7037(01)00653-6), 2001.
- 961 Hedges, J. I., Clark, W. A., Quay, P. D., Richey, J. E., Devol, A. H., and Santos, M.:
 962 Compositions and fluxes of particulate organic material in the Amazon River,
 963 *Limnol Oceanogr*, 31, 717–738, <https://doi.org/10.4319/lo.1986.31.4.0717>,
 964 1986.
- 965 Jetten, M. S. M., Stams, A. J. M., and Zehnder, A. J. B.: Methanogenesis from acetate:
 966 a comparison of the acetate metabolism in *Methanothrix soehngenii* and
 967 *Methanosarcina* spp., *FEMS Microbiol Lett*, 88, 181–198,
 968 <https://doi.org/10.1111/j.1574-6968.1992.tb04987.x>, 1992.
- 969 Kawamura, K., Ishiwatari, R., and Ogura, K.: Early diagenesis of organic matter in
 970 the water column and sediments: Microbial degradation and resynthesis of lipids
 971 in Lake Haruna, *Org Geochem*, 11, 251–264, [https://doi.org/10.1016/0146-6380\(87\)90036-2](https://doi.org/10.1016/0146-6380(87)90036-2), 1987.
- 973 Kristensen, E., Ahmed, S. I., and Devol, A. H.: Aerobic and anaerobic
 974 decomposition of organic matter in marine sediment: Which is fastest?, *Limnol*
 975 *Oceanogr*, 40, 1430–1437, <https://doi.org/10.4319/lo.1995.40.8.1430>, 1995.
- 976 Kuivila, K. M., Murray, J. W., Devol, A. H., and Novelli, P. C.: Methane production,
 977 sulfate reduction and competition for substrates in the sediments of Lake
 978 Washington, *Geochim Cosmochim Acta*, 53, 409–416,
 979 [https://doi.org/10.1016/0016-7037\(89\)90392-X](https://doi.org/10.1016/0016-7037(89)90392-X), 1989.
- 980 Ladd, S. N., Nelson, D. B., Schubert, C. J., and Dubois, N.: Lipid compound classes
 981 display diverging hydrogen isotope responses in lakes along a nutrient gradient,
 982 *Geochim Cosmochim Acta*, 237, 103–119,
 983 <https://doi.org/10.1016/j.gca.2018.06.005>, 2018.
- 984 Lamb, A. L., Wilson, G. P., and Leng, M. J.: A review of coastal palaeoclimate and
 985 relative sea-level reconstructions using $\delta^{13}\text{C}$ and C/N ratios in organic material,
 986 *Earth Sci Rev*, 75, 29–57, <https://doi.org/10.1016/j.earscirev.2005.10.003>, 2006.
- 987 Larsen, S., Andersen, T., and Hessen, D. O.: Climate change predicted to cause
 988 severe increase of organic carbon in lakes, *Glob Chang Biol*, 17, 1186–1192,
 989 <https://doi.org/10.1111/j.1365-2486.2010.02257.x>, 2011.
- 990 Lehmann, M. F., Bernasconi, S. M., Barbieri, A., and McKenzie, J. A.: Preservation
 991 of organic matter and alteration of its carbon and nitrogen isotope composition



992 during simulated and in situ early sedimentary diagenesis, *Geochim Cosmochim*
 993 *Acta*, 66, 3573–3584, [https://doi.org/10.1016/S0016-7037\(02\)00968-7](https://doi.org/10.1016/S0016-7037(02)00968-7), 2002a.
 994 Lehmann, M. F., Bernasconi, S. M., Barbieri, A., and McKenzie, J. A.: Preservation
 995 of organic matter and alteration of its carbon and nitrogen isotope composition
 996 during simulated and in situ early sedimentary diagenesis, *Geochim Cosmochim*
 997 *Acta*, 66, 3573–3584, [https://doi.org/10.1016/S0016-7037\(02\)00968-7](https://doi.org/10.1016/S0016-7037(02)00968-7), 2002b.
 998 Lehmann, M. F., Carstens, D., Deek, A., McCarthy, M., Schubert, C. J., and Zopfi, J.:
 999 Amino acid and amino sugar compositional changes during in vitro degradation
 1000 of algal organic matter indicate rapid bacterial re-synthesis, *Geochim Cosmochim*
 1001 *Acta*, 283, 67–84, <https://doi.org/10.1016/j.gca.2020.05.025>, 2020.
 1002 Lever, M. A. and Teske, A. P.: Diversity of methane-cycling archaea in
 1003 hydrothermal sediment investigated by general and group-specific PCR primers,
 1004 *Appl Environ Microbiol*, 81, 1426–1441, [https://doi.org/10.1128/AEM.03588-](https://doi.org/10.1128/AEM.03588-14)
 1005 14, 2015.
 1006 Li, B., Wang, H., Lai, A., Xue, J., Wu, Q., Yu, C., Xie, K., Mao, Z., Li, H., Xing, P., and
 1007 Wu, Q. L.: Hydrogenotrophic pathway dominates methanogenesis along the
 1008 river-estuary continuum of the Yangtze River, *Water Res*, 240, 120096,
 1009 <https://doi.org/10.1016/j.watres.2023.120096>, 2023.
 1010 Liu, Y. and Whitman, W. B.: Metabolic, Phylogenetic, and Ecological Diversity of
 1011 the Methanogenic Archaea, *Ann N Y Acad Sci*, 1125, 171–189,
 1012 <https://doi.org/10.1196/annals.1419.019>, 2008.
 1013 Liu, Y., Conrad, R., Yao, T., Gleixner, G., and Claus, P.: Change of methane
 1014 production pathway with sediment depth in a lake on the Tibetan plateau,
 1015 *Palaeogeogr Palaeoclimatol Palaeoecol*, 474, 279–286,
 1016 <https://doi.org/10.1016/j.palaeo.2016.06.021>, 2017.
 1017 Lyu, Z., Shao, N., Akinyemi, T., and Whitman, W. B.: Methanogenesis, *Current*
 1018 *Biology*, 28, R727–R732, <https://doi.org/10.1016/j.cub.2018.05.021>, 2018.
 1019 Masson-Delmotte, V., Zhai, P., Pirani, A., Connors, S. L., Péan, C., Berger, S., Caud,
 1020 N., Chen, Y., Goldfarb, L., and Gomis, M. I.: Climate change 2021: the physical
 1021 science basis, Contribution of working group I to the sixth assessment report of
 1022 the intergovernmental panel on climate change, 2, 2391, 2021.
 1023 McMurdie, P. J. and Holmes, S.: Phyloseq: an R package for reproducible
 1024 interactive analysis and graphics of microbiome census data, *PLoS One*, 8, 1–11,
 1025 <https://doi.org/10.1371/journal.pone.0061217>, 2013.
 1026 Meier, D., van Grinsven, S., Michel, A., Eickenbusch, P., Glombitza, C., Han, X.,
 1027 Fiskal, A., Bernasconi, S., Schubert, C. J., and Lever, M. A.: Hydrogen-independent
 1028 CO₂ reduction dominates methanogenesis in five temperate lakes that differ in
 1029 trophic states, *ISME Communications*, 4,
 1030 <https://doi.org/10.1093/ismeco/ycae089>, 2024.
 1031 Mendonça, R., Müller, R. A., Clow, D., Verpoorter, C., Raymond, P., Tranvik, L. J.,
 1032 and Sobek, S.: Organic carbon burial in global lakes and reservoirs, *Nat Commun*,
 1033 8, 1–6, <https://doi.org/10.1038/s41467-017-01789-6>, 2017.
 1034 Meyers, P. A.: Preservation of elemental and isotopic source identification of
 1035 sedimentary organic matter, *Chem Geol*, 114, 289–302,
 1036 [https://doi.org/10.1016/0009-2541\(94\)90059-0](https://doi.org/10.1016/0009-2541(94)90059-0), 1994.
 1037 Meyers, P. A. and Ishiwatari, R.: Lacustrine organic geochemistry-an overview of
 1038 indicators of organic matter sources and diagenesis in lake sediments, *Org*
 1039 *Geochem*, 20, 867–900, [https://doi.org/10.1016/0146-6380\(93\)90100-P](https://doi.org/10.1016/0146-6380(93)90100-P), 1993.



- 1040 Meyers, P. A. and Takeuchi, N.: Environmental changes in Saginaw Bay, Lake
1041 Huron recorded by geolipid contents of sediments deposited since 1800,
1042 *Environmental Geology*, 3, 257–266, <https://doi.org/10.1007/BF02473517>,
1043 1981.
- 1044 O'Leary, M. H.: Carbon isotope fractionation in plants, *Phytochemistry*, 20, 553–
1045 567, [https://doi.org/10.1016/0031-9422\(81\)85134-5](https://doi.org/10.1016/0031-9422(81)85134-5), 1981.
- 1046 Opsahl, S. and Benner, R.: Early diagenesis of vascular plant tissues: Lignin and
1047 cutin decomposition and biogeochemical implications, *Geochim Cosmochim*
1048 *Acta*, 59, 4889–4904, [https://doi.org/10.1016/0016-7037\(95\)00348-7](https://doi.org/10.1016/0016-7037(95)00348-7), 1995.
- 1049 Oren, A.: The Family Methanoregulaceae, in: *The Prokaryotes*, Springer Berlin
1050 Heidelberg, Berlin, Heidelberg, 253–258, https://doi.org/10.1007/978-3-642-38954-2_5, 2014a.
- 1052 Oren, A.: The Family Methanosarcinaceae, in: *The Prokaryotes*, Springer Berlin
1053 Heidelberg, Berlin, Heidelberg, 259–281, https://doi.org/10.1007/978-3-642-38954-2_408, 2014b.
- 1055 Parsons, T. R., Stephens, K., and Strickland, J. D. H.: On the Chemical Composition
1056 of Eleven Species of Marine Phytoplankters, *Journal of the Fisheries Research*
1057 *Board of Canada*, 18, 1001–1016, <https://doi.org/10.1139/f61-063>, 1961.
- 1058 Randlett, M.-E., Sollberger, S., Del Sontro, T., Müller, B., Corella, J. P., Wehrli, B.,
1059 and Schubert, C. J.: Mineralization pathways of organic matter deposited in a
1060 river–lake transition of the Rhone River Delta, Lake Geneva, *Environ Sci Process*
1061 *Impacts*, 17, 370–380, <https://doi.org/10.1039/C4EM00470A>, 2015.
- 1062 Raymond, P. A. and Bauer, J. E.: Riverine export of aged terrestrial organic matter
1063 to the North Atlantic Ocean, *Nature*, 409, 497–500,
1064 <https://doi.org/10.1038/35054034>, 2001.
- 1065 Ritalahti, K. M., Amos, B. K., Sung, Y., Wu, Q., Koenigsberg, S. S., and Löffler, F. E.:
1066 Quantitative PCR targeting 16S rRNA and reductive dehalogenase genes
1067 simultaneously monitors multiple Dehalococcoides strains, *Appl Environ*
1068 *Microbiol*, 72, 2765–2774, <https://doi.org/10.1128/AEM.72.4.2765-2774.2006>,
1069 2006.
- 1070 Rotaru, A.-E., Shrestha, P. M., Liu, F., Shrestha, M., Shrestha, D., Embree, M.,
1071 Zengler, K., Wardman, C., Nevin, K. P., and Lovley, D. R.: A new model for electron
1072 flow during anaerobic digestion: direct interspecies electron transfer to
1073 Methanosaeta for the reduction of carbon dioxide to methane, *Energy Environ.*
1074 *Sci.*, 7, 408–415, <https://doi.org/10.1039/C3EE42189A>, 2014.
- 1075 Schaedler, F., Lockwood, C., Lueder, U., Glombitza, C., Kappler, A., and Schmidt, C.:
1076 Microbially mediated coupling of Fe and N cycles by nitrate-reducing Fe (II)-
1077 oxidizing bacteria in littoral freshwater sediments, *Appl Environ Microbiol*, 84,
1078 1–14, <https://doi.org/10.1128/AEM.02013-17>, 2018.
- 1079 Schellekens, J., Buurman, P., and Pontevedra-Pombal, X.: Selecting parameters for
1080 the environmental interpretation of peat molecular chemistry – A pyrolysis-
1081 GC/MS study, *Org Geochem*, 40, 678–691,
1082 <https://doi.org/10.1016/j.orggeochem.2009.03.006>, 2009.
- 1083 Schubert, C. J. and Nielsen, B.: Effects of decarbonation treatments on $\delta^{13}\text{C}$
1084 values in marine sediments, *Mar Chem*, 72, 55–59,
1085 [https://doi.org/10.1016/S0304-4203\(00\)00066-9](https://doi.org/10.1016/S0304-4203(00)00066-9), 2000.
- 1086 Schulz, S. and Conrad, R.: Effect of algal deposition on acetate and methane
1087 concentrations in the profundal sediment of a deep lake (Lake Constance), *FEMS*



- 1088 Microbiol Ecol, 16, 251–259, [https://doi.org/10.1016/0168-6496\(94\)00088-E](https://doi.org/10.1016/0168-6496(94)00088-E),
1089 1995.
- 1090 Schulz, S. and Conrad, R.: Influence of temperature on pathways to methane
1091 production in the permanently cold profundal sediment of Lake Constance, FEMS
1092 Microbiol Ecol, 20, 1–14, [https://doi.org/10.1016/0168-6496\(96\)00009-8](https://doi.org/10.1016/0168-6496(96)00009-8),
1093 1996.
- 1094 Schwarz, J. I. K. K., Eckert, W., and Conrad, R.: Response of the methanogenic
1095 microbial community of a profundal lake sediment (Lake Kinneret, Israel) to
1096 algal deposition, Limnol Oceanogr, 53, 113–121,
1097 <https://doi.org/10.4319/lo.2008.53.1.0113>, 2008.
- 1098 Shi, W., Sun, M. Y., Molina, M., and Hodson, R. E.: Variability in the distribution of
1099 lipid biomarkers and their molecular isotopic composition in Altamaha estuarine
1100 sediments: Implications for the relative contribution of organic matter from
1101 various sources, Org Geochem, 32, 453–467, [https://doi.org/10.1016/S0146-6380\(00\)00189-3](https://doi.org/10.1016/S0146-6380(00)00189-3), 2001.
- 1103 Smith, K. S. and Ingram-Smith, C.: Methanosaeta, the forgotten methanogen?,
1104 Trends Microbiol, 15, 150–155, <https://doi.org/10.1016/j.tim.2007.02.002>,
1105 2007.
- 1106 Sobek, S., Durisch-Kaiser, E., Zurbrugg, R., Wongfun, N., Wessels, M., Pasche, N.,
1107 and Wehrli, B.: Organic carbon burial efficiency in lake sediments controlled by
1108 oxygen exposure time and sediment source, Limnol Oceanogr, 54, 2243–2254,
1109 <https://doi.org/10.4319/lo.2009.54.6.2243>, 2009.
- 1110 Sobek, S., DelSontro, T., Wongfun, N., and Wehrli, B.: Extreme organic carbon
1111 burial fuels intense methane bubbling in a temperate reservoir, Geophys Res
1112 Lett, 39, 2–5, <https://doi.org/10.1029/2011GL050144>, 2012.
- 1113 Sollberger, S., Corella, J. P., Girardclos, S., Randlett, M. E., Schubert, C. J., Senn, D.
1114 B., Wehrli, B., and DelSontro, T.: Spatial heterogeneity of benthic methane
1115 dynamics in the subaquatic canyons of the Rhone River Delta (Lake Geneva),
1116 Aquat Sci, 76, 89–101, <https://doi.org/10.1007/s00027-013-0319-2>, 2014.
- 1117 Stibal, M., Wadham, J. L., Lis, G. P., Telling, J., Pancost, R. D., Dubnick, A., Sharp, M.
1118 J., Lawson, E. C., Butler, C. E. H., Hasan, F., Tranter, M., and Anesio, A. M.:
1119 Methanogenic potential of Arctic and Antarctic subglacial environments with
1120 contrasting organic carbon sources, Glob Chang Biol, 18, 3332–3345,
1121 <https://doi.org/10.1111/j.1365-2486.2012.02763.x>, 2012.
- 1122 Su, G., Niemann, H., Steinle, L., Zopfi, J., and Lehmann, M. F.: Evaluating
1123 radioisotope-based approaches to measure anaerobic methane oxidation rates in
1124 lacustrine sediments, Limnol Oceanogr Methods, 17, 429–438,
1125 <https://doi.org/10.1002/lom3.10323>, 2019.
- 1126 Su, G., Zopfi, J., Yao, H., Steinle, L., Niemann, H., and Lehmann, M. F.:
1127 Manganese/iron-supported sulfate-dependent anaerobic oxidation of methane
1128 by archaea in lake sediments, Limnol Oceanogr, 65, 863–875,
1129 <https://doi.org/10.1002/lno.11354>, 2020.
- 1130 Su, G., Lehmann, M. F., Tischer, J., Weber, Y., Lepori, F., Walser, J.-C., Niemann, H.,
1131 and Zopfi, J.: Water column dynamics control nitrite-dependent anaerobic
1132 methane oxidation by Candidatus “Methyloirabilis” in stratified lake basins,
1133 ISME J, 17, 693–702, <https://doi.org/10.1038/s41396-023-01382-4>, 2023.
- 1134 Tolu, J., Gerber, L., Boily, J.-F., and Bindler, R.: High-throughput characterization
1135 of sediment organic matter by pyrolysis–gas chromatography/mass
1136 spectrometry and multivariate curve resolution: A promising analytical tool in



- 1137 (paleo)limnology, *Anal Chim Acta*, 880, 93–102,
 1138 <https://doi.org/10.1016/j.aca.2015.03.043>, 2015.
 1139 Tolu, J., Rydberg, J., Meyer-Jacob, C., Gerber, L., and Bindler, R.: Spatial variability
 1140 of organic matter molecular composition and elemental geochemistry in surface
 1141 sediments of a small boreal Swedish lake, *Biogeosciences*, 14, 1773–1792,
 1142 <https://doi.org/10.5194/bg-14-1773-2017>, 2017.
 1143 Valentine, D. W., Holland, E. A., and Schimel, D. S.: Ecosystem and physiological
 1144 controls over methane production in northern wetlands, *J Geophys Res*, 99,
 1145 1563, <https://doi.org/10.1029/93JD00391>, 1994.
 1146 Volkman, J. K.: A review of sterol markers for marine and terrigenous organic
 1147 matter, *Org Geochem*, 9, 83–99, [https://doi.org/10.1016/0146-6380\(86\)90089-](https://doi.org/10.1016/0146-6380(86)90089-6)
 1148 6, 1986.
 1149 Volkman, J. K., Johns, R. B., Gillan, F. T., Perry, G. J., and Bavor, H. J.: Microbial
 1150 lipids of an intertidal sediment—I. Fatty acids and hydrocarbons, *Geochim*
 1151 *Cosmochim Acta*, 44, 1133–1143, [https://doi.org/10.1016/0016-](https://doi.org/10.1016/0016-7037(80)90067-8)
 1152 7037(80)90067-8, 1980.
 1153 Volkman, J. K., Barrett, S. M., Blackburn, S. I., Mansour, M. P., Sikes, E. L., and Gelin, F.: Microalgal biomarkers: A review of recent research developments, *Org*
 1154 *Geochem*, 29, 1163–1179, [https://doi.org/10.1016/S0146-6380\(98\)00062-X](https://doi.org/10.1016/S0146-6380(98)00062-X),
 1155 1998.
 1157 West, W. E., Coloso, J. J., and Jones, S. E.: Effects of algal and terrestrial carbon on
 1158 methane production rates and methanogen community structure in a temperate
 1159 lake sediment, *Freshw Biol*, 57, 949–955, [https://doi.org/10.1111/j.1365-](https://doi.org/10.1111/j.1365-2427.2012.02755.x)
 1160 2427.2012.02755.x, 2012.
 1161 West, W. E., McCarthy, S. M., and Jones, S. E.: Phytoplankton lipid content
 1162 influences freshwater lake methanogenesis, *Freshw Biol*, 2261–2269,
 1163 <https://doi.org/10.1111/fwb.12652>, 2015.
 1164 Whiticar, M. J.: Carbon and hydrogen isotope systematics of bacterial formation
 1165 and oxidation of methane, *Chem Geol*, 161, 291–314,
 1166 [https://doi.org/10.1016/S0009-2541\(99\)00092-3](https://doi.org/10.1016/S0009-2541(99)00092-3), 1999.
 1167 Whiticar, M. J. J., Faber, E., and Schoell, M.: Biogenic methane formation in marine
 1168 and freshwater environments: CO₂ reduction vs. acetate fermentation—Isotope
 1169 evidence, *Geochim Cosmochim Acta*, 50, 693–709,
 1170 [https://doi.org/10.1016/0016-7037\(86\)90346-7](https://doi.org/10.1016/0016-7037(86)90346-7), 1986.
 1171 Xiao, K.-Q., Beulig, F., Røy, H., Jørgensen, B. B., and Risgaard-Petersen, N.:
 1172 Methylophilic methanogenesis fuels cryptic methane cycling in marine surface
 1173 sediment, *Limnol Oceanogr*, 63, 1519–1527, <https://doi.org/10.1002/lno.10788>,
 1174 2018.
 1175 Xu, L., Zhuang, G. C., Montgomery, A., Liang, Q., Joye, S. B., and Wang, F.: Methyl-
 1176 compounds driven benthic carbon cycling in the sulfate-reducing sediments of
 1177 South China Sea, *Environ Microbiol*, 23, 641–651,
 1178 <https://doi.org/10.1111/1462-2920.15110>, 2021.
 1179 Zhao, B., Ma, J., Zhao, Q., Laurens, L., Jarvis, E., Chen, S., and Frear, C.: Efficient
 1180 anaerobic digestion of whole microalgae and lipid-extracted microalgae residues
 1181 for methane energy production, *Bioresour Technol*, 161, 423–430,
 1182 <https://doi.org/10.1016/j.biortech.2014.03.079>, 2014.
 1183 Zhou, J., Smith, J. A., Li, M., and Holmes, D. E.: Methane production by
 1184 *Methanothrix thermoacetophila* via direct interspecies electron transfer with



1185 *Geobacter metallireducens*, mBio, 2–3, <https://doi.org/10.1128/mbio.00360-23>,
1186 2023.
1187 Zhuang, G.-C., Heuer, V. B., Lazar, C. S., Goldhammer, T., Wendt, J., Samarkin, V. A.,
1188 Elvert, M., Teske, A. P., Joye, S. B., and Hinrichs, K.-U.: Relative importance of
1189 methylotrophic methanogenesis in sediments of the Western Mediterranean Sea,
1190 *Geochim Cosmochim Acta*, 224, 171–186,
1191 <https://doi.org/10.1016/j.gca.2017.12.024>, 2018.
1192